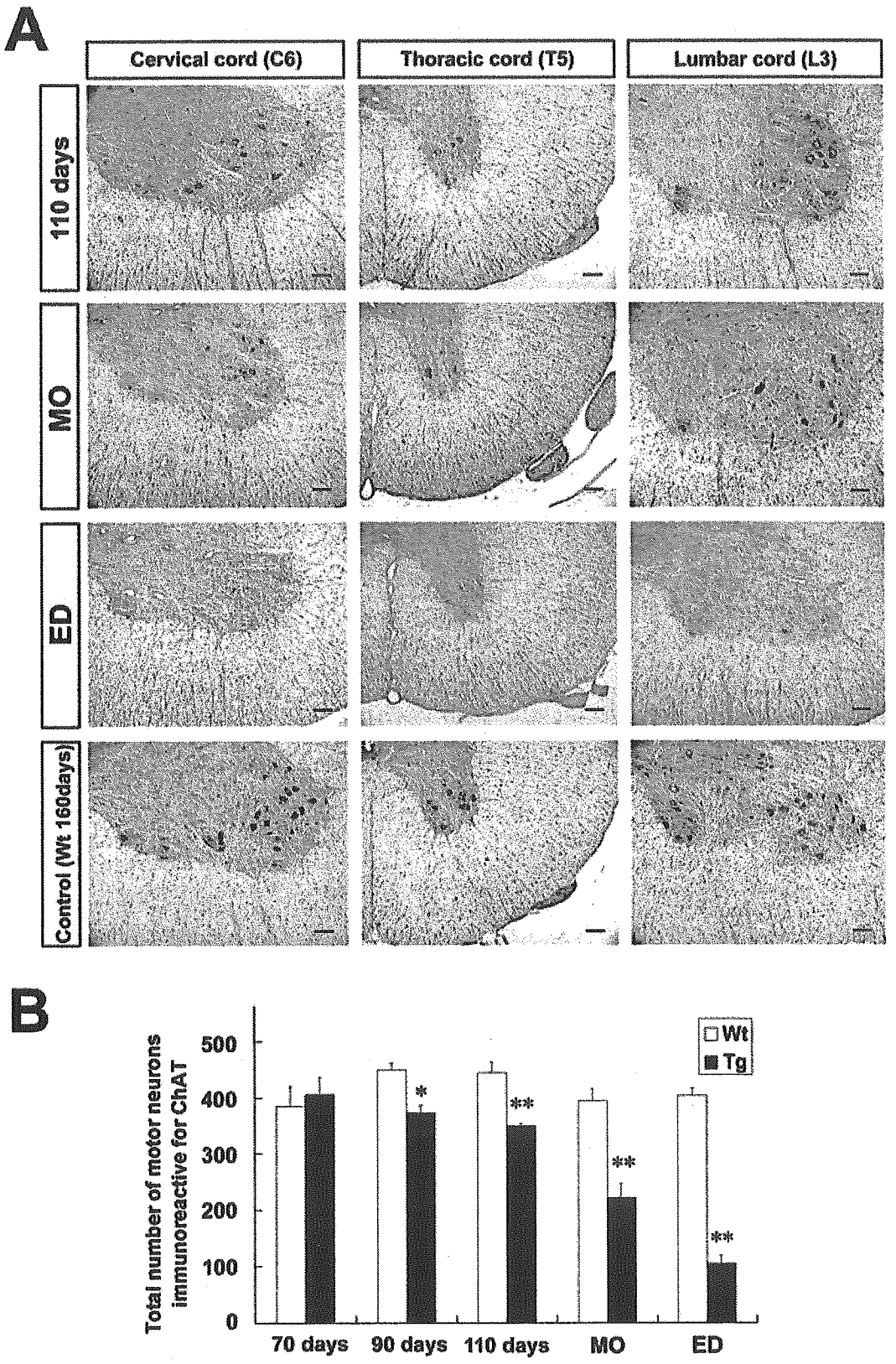

Fig. 7. The loss of motor neurons in the spinal cord of hSOD1 (G93A) transgenic rats at different stages. **A:** Immunohistochemical analysis of the spinal cord of transgenic rats. Transverse sections of the cervical (C6), thoracic (T5), and lumbar (L3) spinal cord of the transgenic rats and their wild-type littermates were stained with an anti-ChAT antibody to label viable motor neurons at the indicated stages (Scale bars = 100 μm). **B:** The number of ChAT immunoreactive motor neurons was counted and is shown in the histograms as the total number of motor neurons in the C6, T5, and L3 segments. This number began to decrease in the transgenic rats at 90 days of age, rapidly declined after 110 days of age, and fell to about 50% and 25% of wild-type rats at the muscle weakness onset (MO, around 125 days) and at end-stage disease (ED, around 140 days), respectively. Bars = means ± SEM ($n = 3$ for each genotype). $^{*}P < 0.05$. $^{**}P < 0.01$; two-tailed unpaired Student's t-test.

of their wild-type littermates at 70, 90, and 110 days of age, when the transgenic rats scored <70° in the inclined plane test (muscle weakness onset), and failed the righting reflex. To quantify the number of spinal motor neurons, we stained spinal cord sections of both groups with an anti-ChAT antibody.

As shown in Figure 7A, the numbers of ChAT immunoreactive motor neurons in the cervical (C6), thoracic (T5), and lumbar (L3) segments of the spinal cord decreased with disease progression. Quantitative analysis of the residual motor neurons showed that the total number of motor neurons in the transgenic rats began to decrease at 90 days of age, rapidly declined after 110 days of age, and fell to about 50% and 25% of the numbers in age-matched wild-type littermates at the time the score was <70° in the inclined plane test (muscle weakness onset) and of righting reflex failure, respectively (Fig. 7B).

DISCUSSION

Factors Underlying the Variability in Phenotypes of hSOD1 (G93A) Transgenic Rats

In previous studies of this G93A rat, only the hindlimb-type has been described, and the variety of phenotypes and variable clinical courses have not yet been mentioned (Nagai et al., 2001). Recently, however, another line of G93A rats backcrossed onto a Wistar background ($SOD1^{G93A/HWr}$ rats) was reported to present two phenotypes, including forelimb-type, and a large inter-litter variability in disease onset (Storkebaum et al., 2005). In the same way, commonly used FALS model mice harboring hSOD1 (G93A) gene have been reported to have clinical variability to some extent, and some of them dominantly show forelimb paralysis (Gurney et al., 1994). In this study, we recognized various clinical types, including forelimb-, hindlimb-, and general-type and established quantitative methods to evaluate disease progression that can be applied to any of the clinical types of this ALS model. We have also shown the variability in disease progression to depend on clinical types, that is, disease progression after the onset was faster in forelimb-type than in hindlimb-type rats. This difference may be due to the aggressiveness of the disease per se because we evaluated the time point of "death" (end-stage disease) according to righting reflex failure (Howland et al., 2002) to exclude the influence of feeding problems (bulbar region) and respiratory failure (level C2–C4).

These findings give rise to the next question; why is this variety of phenotypes and variability in the clinical course observed in the same transgenic line? There are at least three possible explanations. One is that the variation is due to the heterogeneous genetic background of the Sprague-Dawley (SD) rat (i.e., the strain used to generate this transgenic line), which might have led to different phenotypes. This idea is supported by the fact that the SD strain shows a large inter-individual disease variability in other models of neurodegenerative disorders, such as Huntington's disease (Ouary et al., 2000). Similar phenotypic variability takes place in human FALS carrying the same mutations in hSOD1 gene (Abe et al., 1996; Watanabe et al., 1997; Kato et al., 2001), which could be explained by heterogeneous genetic backgrounds. Thus, the present transgenic ALS model rats may be highly useful to understand the mechanisms of bulbar onset, arm onset, or leg onset that are seen in human disease. There may be modifier genes of these phenotypes, which should be identified in the future study.

TABLE VI. Adequacy of Evaluation Methods in Regard to Practical Use*

	Body weight	Inclined plane	Cage activity	SCANET	Motor score
Objectivity	A	B	A	A	B
Sensitivity	A	B	C	(A)	-
Specificity	C	B	C	C	A
Motivation independence	A	B	B	D	B
Skill requirements	A	B	A	A	B
Cost of apparatus	B	B	D	D	A

*A, more appropriate; B, appropriate; C, less appropriate; D, inappropriate.

The second is that there is variability in the expression of the mutant hSOD1 protein. The transcriptional regulation of this exogenous gene could be affected by one or more unknown factors, such as epigenetic regulation, and may not be expressed uniformly throughout the spinal cord of each animal. Therefore, some rats might express mutant proteins more in the cervical spinal cord and others might express more in the lumber cord, possibly resulting in the forelimb type and hindlimb type, respectively. However, we found no definite correlation between local expression levels of the mutant hSOD1 mRNA/protein in the spinal cord and the phenotypes of these animals, using real time RT-PCR and western blot analysis after the onset of muscle weakness, when the clinical type of the transgenic rats could be defined (Fig. 6). Moreover, the pathological analysis showed no correlation between the number of residual motor neurons in each segment and the phenotypes of end-stage animals. However, because >50% of spinal motor neurons have already degenerated at the stage of muscle weakness onset, whether local expression of the mutant hSOD1 gene and segmental loss of motor neurons correlate with the clinical types of G93A rats should be further investigated by analyzing younger animals at a stage when motor neuron loss has not progressed as much.

The third explanation involves a structural property of the mutant hSOD1 (G93A) protein itself. It is now thought that mutations in the hSOD1 gene may alter the 3-D conformation of the enzyme and, in turn, result in the SOD1 protein acquiring toxic properties that cause ALS (Deng et al., 1993; Hand and Rouleau 2002). For instance, the hSOD1 (G93A) mutant protein has been reported to be susceptible to nonnative protein–protein interactions because of its mutation site and unfolded structure (Shipp et al., 2003; Furukawa and

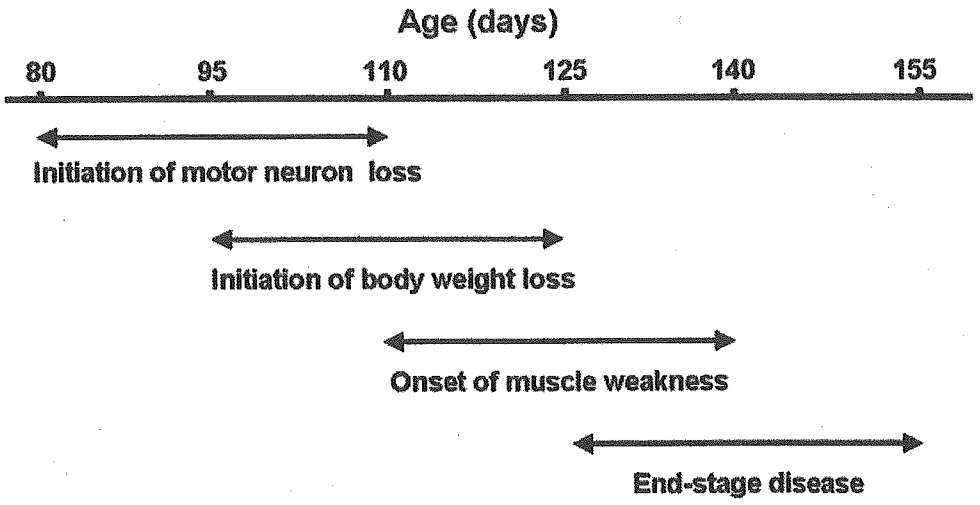

Fig. 8. Four stages of disease progression in hSOD1 (G93A) transgenic rats. The disease progression can be classified into four stages as shown. The range for each stage is about 1 month and overlaps approximately 2 weeks with the next stage.

O'Halloran, 2005), suggesting that the G93A mutation might accelerate the formation of SOD1 protein aggregates, which may ultimately sequester heat-shock proteins and molecular chaperones, disturb axonal transport or protein degradation machineries, including the ubiquitin-proteasome system (Borchelt et al., 1998; Bruening et al., 1999; Williamson and Cleveland 1999; Okado-Matsumoto and Fridovich 2002; Urushitani et al., 2002). Curiously, the mutated hSOD1 (G93A) protein is more susceptible to degradation by the ubiquitin-proteasome system and has a shorter half-life than other mutants (Fujiwara et al., 2005), suggesting that it may cause more unstable toxic aggregates in the spinal cord than other mutations. The degradation rate is also affected by environmental factors unique to each animal, such as the progressive decline of proteasome function with age (Keller et al., 2000), and these factors could contribute to the variability of the clinical course of G93A rats.

Taking all these findings into consideration, the mutated hSOD1 (G93A) protein may gain properties that are responsible for a variety of phenotypes and variability in the clinical course of the affected animals.

Characteristics of Different Methods for Assessing hSOD1 (G93A) Transgenic Rats

The ideal measure is not influenced by the judgment of the observer, sensitive to small abnormalities, specific to detect pathologic events that are related to pathogenesis of the ALS-like disease, not influenced by the motivational factors of rats, minimal in the requirements for skill in the observer, and inexpensive to carry out. We assessed each evaluation method by the categories in regard to practical use as shown in the Table 6.

The initiation of body weight loss seems to be an excellent marker to detect the onset and should be highly recommended. Muscle volume might have already started to decrease, even in the period of continuous weight gain, as reported for hSOD1 (G93A) transgenic mice (Brooks et al., 2004). As a result, it could detect an abnormality relatively earlier than subjective onset. The inclined plane test is considered to be the least defective method of all. It could objectively and specifically detect the decline in the muscle strength of these ALS model rats as a muscle weakness onset almost at the same time of the subjective onset. The cage activity measurement and SCANET require very expensive apparatus, and are limited by the availability of funds and space for making the measurements. Although SCANET test was most sensitive among these measures, it seems inappropriate for the statistical analysis, and does not add any more information than that obtained through simple observation of the rats because the performances of the rats might be severely affected by the extent of their motivation to explore. Motor score can specifically assess disease progression of each clinical type and is valuable in keeping the experimental costs at a minimum.

Correlation Between the Loss of Spinal Motor Neurons and Disease Stages

This study clearly shows the variable clinical course of G93A rats. According to our behavioral and histological analyses, we can divide the disease course of this transgenic model into four stages, whose durations have a range of about 1 month, as shown in Figure 8. Furthermore, we have established the pathological validity of the performance deficits detected by each measure of disease progression. "Initiation of motor neuron loss" was defined as a statistically significant decrease in the number of spinal motor neurons, which was found at around 90 days of age, but not 70 days of age (Fig. 7B). This coincides with, and seems to be sensitively detected by the marked difference in SCANET scores that begins at around 90 days of age (Fig. 3D–F). The "initiation of body weight loss" was usually detected at around 110 days of age as the peak body weight (pre-symptomatic onset, 113.6 ± 4.8 days of age, range = 103–124, Table IV). This stage coincides with the initiation of a rapid decline in the number of motor neurons at around 110 days of age (Fig. 7B). "Onset of muscle weakness" was detected at around 125 days of age, as assessed by the

inclined plane test (muscle weakness onset, 125.2 ± 7.4 days of age, range = 110–144, Table IV). This coincides with the number of spinal motor neurons in the transgenic rats being reduced to about 50% of the number in wild-type rats (Fig. 7B). We presume that transgenic rats do not present obvious muscle weakness until the number of motor neurons has been reduced to approximately half the number found in the healthy state. "End-stage disease" as defined by righting reflex failure was recorded at around 140 days of age (137.8 ± 7.1 days of age, range = 122–155, Table IV). At this stage, the affected rats had only about 25% of the spinal motor neurons of age- and gender-matched wild-type rats (Fig. 7B), and showed a generalized loss of motor activity. Thus, our findings allow us to estimate the extent of spinal motor neuron loss by evaluating the disease stage with the measures described in this study.

In summary, we have described the variable phenotypes of mutant hSOD1 (G93A) transgenic rats and established an evaluation system applicable to all clinical types of these rats. Disease stages defined by this evaluation system correlated well pathologically with the reduction of motor neurons. Our evaluation system of this animal model should be a valuable tool for future preclinical experiments aimed at developing novel treatments for ALS.

ACKNOWLEDGMENTS

We thank Dr. H.-N. Dai of the Department of Neuroscience, Georgetown University School of Medicine for technical advice and valuable discussions, and Dr. T. Yoshizaki and Miss K. Kaneko for participating in the assessment of transgenic rats with the Motor score. This work was supported by grants from CREST, Japan Society for the Promotion of Science to H.O., a Research Grant on Measures for Intractable Diseases from the Japanese Ministry of Health, Labour and Welfare to H.O., M.A., G.S. and Y.I., and a Grant-in-Aid for the 21st century COE program to Keio University from the Japanese Ministry of Education, Culture, Sports, Science and Technology.

REFERENCES

Abe K, Aoki M, Ikeda M, Watanabe M, Hirai S, Itoyama Y. 1996. Clinical characteristics of familial amyotrophic lateral sclerosis with Cu/Zn superoxide dismutase gene mutations. J Neurol Sci 136:108–116.

Azzouz M, Ralph GS, Storkebaum E, Walmsley LE, Mitrophanous KA, Kingsman SM, Carmeliet P, Mazarakis ND. 2004. VEGF delivery with retrogradely transported lentivector prolongs survival in a mouse ALS model. Nature 429:413–417.

Barneoud P, Lolivier J, Sanger DJ, Scatton B, Moser P. 1997. Quantitative motor assessment in FALS mice: a longitudinal study. Neuroreport 8:2861–2865.

Borchelt DR, Wong PC, Becher MW, Pardo CA, Lee MK, Xu ZS, Thinakaran G, Jenkins NA, Copeland NG, Sisodia SS, Cleveland DW, Price DL, Hoffman PN. 1998. Axonal transport of mutant superoxide dismutase 1 and focal axonal abnormalities in the proximal axons of transgenic mice. Neurobiol Dis 5:27–35.

Brooks KJ, Hill MD, Hockings PD, Reid DG. 2004. MRI detects early hindlimb muscle atrophy in Gly93Ala superoxide dismutase-1 (G93A SOD1) transgenic mice, an animal model of familial amyotrophic lateral sclerosis. NMR Biomed 17:28–32.

Brown RH Jr. 1995. Amyotrophic lateral sclerosis: recent insights from genetics and transgenic mice. Cell 80:687–692.

Bruening W, Roy J, Giasson B, Figlewicz DA, Mushynski WE, Durham HD. 1999. Up-regulation of protein chaperones preserves viability of cells expressing toxic Cu/Zn-superoxide dismutase mutants associated with amyotrophic lateral sclerosis. J Neurochem 72:693–699.

Chiu AY, Zhai P, Dal Canto MC, Peters TM, Kwon YW, Prattis SM, Gurney ME. 1995. Age-dependent penetrance of disease in a transgenic mouse model of familial amyotrophic lateral sclerosis. Mol Cell Neurosci 6:349–362.

de Belleroche J, Orrell R, King A. 1995. Familial amyotrophic lateral sclerosis/motor neurone disease (FALS): a review of current developments. J Med Genet 32:841–847.

Deng HX, Hentati A, Tainer JA, Iqbal Z, Cayabyab A, Hung WY, Getzoff ED, Hu P, Herzfeldt B, Roos RP, Warner C, Deng G, Soriano E, Smyth C, Parge HE, Ahmed A, Roses AD, Hallewell RA, Pericak-Vance MA, Siddique T. 1993. Amyotrophic lateral sclerosis and structural defects in Cu, Zn superoxide dismutase. Science 261:1047–1051.

Fujiwara N, Miyamoto Y, Ogasahara K, Takahashi M, Ikegami T, Takamiya R, Suzuki K, Taniguchi N. 2005. Different immunoreactivity against monoclonal antibodies between wild-type and mutant copper/zinc superoxide dismutase linked to amyotrophic lateral sclerosis. J Biol Chem 280:5061–5070.

Furukawa Y, O'Halloran TV. 2005. Amyotrophic lateral sclerosis mutations have the greatest destabilizing effect on the Apo- and reduced form of SOD1, leading to unfolding and oxidative aggregation. J Biol Chem 280:17266–17274.

Gale K, Kerasidis H, Wrathall JR. 1985. Spinal cord contusion in the rat: behavioral analysis of functional neurologic impairment. Exp Neurol 88:123–134.

Garbuzova-Davis S, Willing AE, Milliken M, Saporta S, Zigova T, Cahill DW, Sanberg PR. 2002. Positive effect of transplantation of hNT neurons (NTera 2/D1 cell-line) in a model of familial amyotrophic lateral sclerosis. Exp Neurol 174:169–180.

Gurney ME, Pu H, Chiu AY, Dal Canto MC, Polchow CY, Alexander DD, Caliendo J, Hentati A, Kwon YW, Deng HX, Chen W, Zhai F, Sufit RL, Siddique T. 1994. Motor neuron degeneration in mice that express a human Cu,Zn superoxide dismutase mutation. Science 264:1772–1775.

Hand CK, Rouleau GA. 2002. Familial amyotrophic lateral sclerosis. Muscle Nerve 25:135–159.

Howland DS, Liu J, She Y, Goad B, Maragakis NJ, Kim B, Erickson J, Kulik J, DeVito L, Psaltis G, DeGennaro LJ, Cleveland DW, Rothstein JD. 2002. Focal loss of the glutamate transporter EAAT2 in a transgenic rat model of SOD1 mutant-mediated amyotrophic lateral sclerosis (ALS). Proc Natl Acad Sci USA 99:1604–1609.

Inoue H, Tsukita K, Iwasato T, Suzuki Y, Tomioka M, Tateno M, Nagao M, Kawata A, Saido TC, Miura M, Misawa H, Itohara S, Takahashi R. 2003. The crucial role of caspase-9 in the disease progression of a transgenic ALS mouse model. EMBO J 22:6665–6674.

Kaspar BK, Llado J, Sherkat N, Rothstein JD, Gage FH. 2003. Retrograde viral delivery of IGF-1 prolongs survival in a mouse ALS model. Science 301:839–842.

Kato M, Aoki M, Ohta M, Nagai M, Ishizaki F, Nakamura S, Itoyama Y. 2001. Marked reduction of the Cu/Zn superoxide dismutase polypeptide in a case of familial amyotrophic lateral sclerosis with the homozygous mutation. Neurosci Lett 312:165–168.

Keller JN, Huang FF, Zhu H, Yu J, Ho YS, Kindy TS. 2000. Oxidative stress-associated impairment of proteasome activity during ischemia-reperfusion injury. J Cereb Blood Flow Metab 20:1467–1473.

Landis JR, Koch GG. 1977. The measurement of observer agreement for categorical data. Biometrics 33:159–174.

Mikami Y, Toda M, Watanabe M, Nakamura M, Toyama Y, Kawakami Y. 2002. A simple and reliable behavioral analysis of locomotor function after spinal cord injury in mice. Technical note. J Neurosurg Spine 97:142–147.

Mulder DW, Kurland LT, Offord KP, Beard CM. 1986. Familial adult motor neuron disease: amyotrophic lateral sclerosis. Neurology 36:511–517.

Nagai M, Aoki M, Miyoshi I, Kato M, Pasinelli P, Kasai N, Brown RH, Jr., Itoyama Y. 2001. Rats expressing human cytosolic copper-zinc superoxide dismutase transgenes with amyotrophic lateral sclerosis: associated mutations develop motor neuron disease. J Neurosci 21:9246–9254.

Ohki-Hamazaki H, Sakai Y, Kamata K, Ogura H, Okuyama S, Watase K, Yamada K, Wada K. 1999. Functional properties of two bombesin-like peptide receptors revealed by the analysis of mice lacking neuromedin B receptor. J Neurosci 19:948–954.

Okada Y, Shimazaki T, Sobue G, Okano H. 2004. Retinoic-acid-concentration-dependent acquisition of neural cell identity during in vitro differentiation of mouse embryonic stem cells. Dev Biol 275:124–142.

Okado-Matsumoto A, Fridovich I. 2002. Amyotrophic lateral sclerosis: a proposed mechanism. Proc Natl Acad Sci USA 99:9010–9014.

Ouary S, Bizat N, Altairac S, Menetrat H, Mittoux V, Conde F, Hantraye P, Brouillet E. 2000. Major strain differences in response to chronic systemic administration of the mitochondrial toxin 3-nitropropionic acid in rats: implications for neuroprotection studies. Neuroscience 97:521–530.

Rivlin AS, Tator CH. 1977. Objective clinical assessment of motor function after experimental spinal cord injury in the rat. J Neurosurg 47: 577–581.

Rosen DR, Siddique T, Patterson D, Figlewicz DA, Sapp P, Hentati A, Donaldson D, Goto J, O'Regan JP, Deng HX, Rahmani Z, Krizus A, McKenna-Yasek D, Cayabyab A, Gasten SM, Berger R, Tanzi RE, Halperin JJ, Herzfeldt B, van den Bergh R, Hung WY, Bird T, Deng G, Mulder DW, Smyth C, Laing NG, Soriano E, Pericak-Vance MA, Haines J, Reuleau GA, Gusella JS, Horvitz HR, Brown RH Jr. 1993. Mutations in Cu/Zn superoxide dismutase gene are associated with familial amyotrophic lateral sclerosis. Nature 362:59–62.

Shipp EL, Cantini F, Bertini I, Valentine JS, Banci L. 2003. Dynamic properties of the G93A mutant of copper-zinc superoxide dismutase as detected by NMR spectroscopy: implications for the pathology of familial amyotrophic lateral sclerosis. Biochemistry 42:1890–1899.

Storkebaum E, Lambrechts D, Dewerchin M, Moreno-Murciano MP, Appelmans S, Oh H, Van Damme P, Rutten B, Man WY, De Mol M, Wyns S, Manka D, Vermeulen K, Van Den Bosch L, Mertens N, Schmitz C, Robberecht W, Conway EM, Collen D, Moons L, Carmeliet P. 2005. Treatment of motoneuron degeneration by intracerebroventricular delivery of VEGF in a rat model of ALS. Nat Neurosci 8:85–92.

Sun W, Funakoshi H, Nakamura T. 2002. Overexpression of HGF retards disease progression and prolongs life span in a transgenic mouse model of ALS. J Neurosci 22:6537–6548.

Urushitani M, Kurisu J, Tsukita K, Takahashi R. 2002. Proteasomal inhibition by misfolded mutant superoxide dismutase 1 induces selective motor neuron death in familial amyotrophic lateral sclerosis. J Neurochem 83:1030–1042.

Wang LJ, Lu YY, Muramatsu S, Ikeguchi K, Fujimoto K, Okada T, Mizukami H, Matsushita T, Hanazono Y, Kume A, Nagatsu T, Ozawa K, Nakano I. 2002. Neuroprotective effects of glial cell line-derived neurotrophic factor mediated by an adeno-associated virus vector in a transgenic animal model of amyotrophic lateral sclerosis. J Neurosci 22: 6920–6928.

Watanabe M, Aoki M, Abe K, Shoji M, Iizuka T, Ikeda Y, Hirai S, Kurokawa K, Kato T, Sasaki H, Itoyama Y. 1997. A novel missense point mutation (S134N) of the Cu/Zn superoxide dismutase gene in a patient with familial motor neuron disease. Hum Mutat 9:69–71.

Weydt P, Hong SY, Kliot M, Moller T. 2003. Assessing disease onset and progression in the SOD1 mouse model of ALS. Neuroreport 14: 1051–1054.

Williamson TL, Cleveland DW. 1999. Slowing of axonal transport is a very early event in the toxicity of ALS-linked SOD1 mutants to motor neurons. Nat Neurosci 2:50–56.

Available online at www.sciencedirect.com
SCIENCE DIRECT®
Neuroscience Research 54 (2006) 11–14
Neuroscience Research
www.elsevier.com/locate/neures

Underediting of GluR2 mRNA, a neuronal death inducing molecular change in sporadic ALS, does not occur in motor neurons in ALS1 or SBMA

Yukio Kawahara [a,1], Hui Sun [a], Kyoko Ito [a], Takuto Hideyama [a], Masashi Aoki [b], Gen Sobue [c], Shoji Tsuji [a], Shin Kwak [a,*]

[a] *Department of Neurology, Graduate School of Medicine, The University of Tokyo, 7-3-1 Hongo, Bunkyo-ku, Tokyo 113-8655, Japan*
[b] *Department of Neurology, Tohoku University Graduate School of Medicine, Sendai, Japan*
[c] *Department of Neurology, Nagoya University Graduate School of Medicine, Nagoya, Japan*

Received 7 July 2005; accepted 13 September 2005
Available online 12 October 2005

Abstract

Deficient RNA editing of the AMPA receptor subunit GluR2 at the Q/R site is a primary cause of neuronal death and recently has been reported to be a tightly linked etiological cause of motor neuron death in sporadic amyotrophic lateral sclerosis (ALS). We quantified the RNA editing efficiency of the GluR2 Q/R site in single motor neurons of rats transgenic for mutant human Cu/Zn-superoxide dismutase (SOD1) as well as patients with spinal and bulbar muscular atrophy (SBMA), and found that GluR2 mRNA was completely edited in all the motor neurons examined. It seems likely that the death cascade is different among the dying motor neurons in sporadic ALS, familial ALS with mutant SOD1 and SBMA.

Keywords: ALS; SOD1; Spinal and bulbar muscular atrophy; Motor neuron; RNA editing; GluR2; AMPA receptor; Neuronal death

1. Introduction

Amyotrophic lateral sclerosis (ALS) is a progressive neurodegenerative disease with selective loss of both upper and lower motor neurons, and familial cases are rare. The etiology of sporadic ALS remains elusive but recently deficient RNA editing of AMPA receptor subunit GluR2 at the Q/R site is reported in motor neurons in ALS that occurs in a disease-specific and motor neuron-selective manner (Kawahara et al., 2004; Kwak and Kawahara, 2005). Moreover, underediting of the GluR2 Q/R site greatly increases the Ca^{2+} permeability of AMPA receptors (Hume et al., 1991; Verdoorn et al., 1991; Burnashev et al., 1992), which may cause neuronal death due to increased Ca^{2+} influx through the receptor channel, hence mice with RNA editing deficiencies at the GluR2 Q/R site die young (Brusa et al., 1995) and mice transgenic for an artificial Ca^{2+}-permeable GluR2 develop motor neuron disease 12 months after birth (Kuner et al., 2005). Such evidence lends strong support to the close relevance of deficient RNA editing of the GluR2 at the Q/R site to death of motor neurons in sporadic ALS. However, although we and other researchers have demonstrated that dying neurons in several neurodegenerative diseases exhibit edited GluR2 (Kwak and Kawahara, 2005), it has not yet been demonstrated whether the underediting of GluR2 occurs in dying motor neurons in motor neuron diseases other than ALS. Such investigation is of particular importance since it will help clarify whether the molecular mechanism of motor neurons death is common among various subtypes of motor neurons.

ALS associated with the SOD1 mutation (ALS1) is the most frequent familial ALS (Rosen et al., 1993), and mutated human SOD1 transgenic animals have been studied extensively as a disease model of ALS1, yet the etiology of neuronal death in the animals has not been elucidated. Another example of non-ALS motor neuron disease is spinal and bulbar muscular atrophy (SBMA), which predominantly affects lower motor neurons with a relatively slow clinical course. Since the CAG

* Corresponding author. Tel.: +81 3 5800 8672; fax: +81 3 5800 6548.
E-mail address: kwak-tky@umin.ac.jp (S. Kwak).
[1] Present address: The Wistar Institute, Philadelphia, PA, USA.

0168-0102/$ – see front matter
doi:10.1016/j.neures.2005.09.006

Table 1
RNA editing efficiency of single motor neurons in SBMA

Case	Age at death (year)	Sex	No. of CAG repeats[a]	Postmortem delay (h)	GluR2(+) MN[b]	MN with 100% editing efficiency (% of GluR2(+) MN)
SBMA, case 1	71	M	48	2.5	12	12 (100)
SBMA, case 2	78	M	42	2.5	16	16 (100)
SBMA, case 3	60	M	44	1	16	16 (100)

[a] Number of CAG repeats in the androgen receptor gene.
[b] Motor neurons in which GluR2 RT-PCR amplifying product was detected.

repeat expansion in the androgen receptor gene has been demonstrated in SBMA (La Spada et al., 1991), and pharmacological castration is therapeutically effective in animal models (Katsuno et al., 2002, 2003), the death cascade responsible for SBMA is likely different from sporadic ALS. In this paper, an investigation is carried out into whether or not the dying mechanism underlying sporadic ALS is the same as ALS1 and SBMA by determining the editing status of the GluR2 Q/R site in single motor neurons.

2. Materials and methods

The animals used in this study were SOD1^{G93A} and SOD1^{H46R} transgenic male rats (Nagai et al., 2001) ($n = 3$ each) that had exhibited progressive neuromuscular weakness with their littermates as the control ($n = 3$ each) (Table 2). The first sign of disease in these rats was weakness of their hindlimbs, mostly exhibited by the dragging of one limb. Onset of motor neuron disease was scored as the first observation of abnormal gait or evidence of limb weakness. The mean age of onset of clinical weakness for the SOD1^{G93A} and SOD1^{H46R} lines was 122.9 ± 14.1 and 144.7 ± 6.4 days, respectively. As the disease progressed, the rats exhibited marked muscle wasting in their hindlimbs, and then in the forelimbs. The mean duration after the clinical expression of the disease in the SOD1^{G93A} and SOD1^{H46R} lines was 8.3 ± 0.7 and 24.2 ± 2.9 days, respectively (Nagai et al., 2001). The rats were killed 3 days and 2 weeks after the onset for the SOD1^{G93A} and SOD1^{H46R} lines, respectively, and we examined their fifth lumbar cord. Animals were handled according to Institutional Animal Care and Use Committee approved protocols that are in line with the Guideline for Animal Care and Use by the National Institute of Health. Spinal cords were isolated after deep pentobarbiturate anesthesia. In addition, spinal cords were obtained at autopsy from three genetically confirmed patients with SBMA (Table 1). Written informed consent was obtained from all subjects prior to death or from their relatives, and the Ethics Committees of Graduate School of Medicine, the University of Nagoya and the University of Tokyo approved the experimental procedures used. Spinal cords were rapidly frozen on dry ice and maintained at −80 °C until use.

Table 2
RNA editing efficiency of single motor neurons in mutated human SOD1 transgenic rats

Case (n)	GluR2(+) MN[a]	MN with 100% editing efficiency (% of GluR2(+) MN)
SOD1^{G93A}-1	13	13 (100)
SOD1^{G93A}-2	21	21 (100)
SOD1^{G93A}-3	21	21 (100)
SOD1^{H46R}-1	19	19 (100)
SOD1^{H46R}-2	23	23 (100)
SOD1^{H46R}-3	20	20 (100)
SOD1^{G93A}, littermates (3)	22	22 (100)
SOD1^{H46R}, littermates (3)	20	20 (100)

[a] Motor neurons in which GluR2 RT-PCR amplifying product was detected.

Single motor neurons were isolated and collected into respective single test tubes that contained 200 μl of TRIZOL Reagent (Invitrogen Corp., Carlsbad, CA, USA) using a laser microdissection system as previously described (Kawahara et al., 2003b, 2004) (LMD, Leica Microsystems Ltd., Germany) (Fig. 1a). After extracting total RNA from single neuron tissue, we analyzed the RNA editing efficiency at the GluR2 Q/R site by means of RT-PCR coupled with digestion of the PCR amplified products with a restriction enzyme Bbv-I (New England BioLabs, Beverly, MA, USA) (Takuma et al., 1999; Kawahara et al., 2003a, 2004), and the editing efficiency was calculated by quantitatively analyzing the digests with a 2100 Bioanalyser (Agilent Technologies, Palo Alto, CA, USA), as previously described (Kawahara et al., 2003a). Briefly, after gel purification using Zymoclean Gel DNA Recovery Kit according to the manufacturer's protocol (Zymo Research, Orange, CA, USA), PCR products were quantified using a 2100 Bioanalyser. An aliquot (0.5 μg) was then incubated at 37 °C for 12 h with 10 × restriction buffer and 2 U of *Bbv*I in a total volume of 20 μl and inactivated at 65 °C for 30 min. The PCR products had one intrinsic *Bbv*I recognition sites, whereas the products originating from unedited GluR2 mRNA had an additional recognition site. Thus, restriction digestion of the PCR products originating from edited rat (278 bp) and human (182 bp) GluR2 mRNA should produce two bands (human GluR2 in parenthesis) at 219 (116) and 59 (66) bp, whereas those originating from unedited GluR2 mRNA should produce three bands at 140 (81), 79 (35), and 59 (66) bp. As the 59 (66) bp band would originate from both edited and unedited mRNA, but the 219 (116) bp band would originate from only edited mRNA, we quantified the molarity of the 219 (116) and 59 (66) bp bands using the 2100 Bioanalyser and calculated the editing efficiency as the ratio of the former to the latter for each sample.

The following primers were used for PCR for rat and human GluR2 (amplified product lengths are also indicated): for rat GluR2 (278 bp): rF (5′-AGCAGATTTAGCCCCTACGAG-3′) and rR (5′-CAGCACTTTCGATGGGAGACAC-3′). for human GluR2, the first PCR (187 bp): hG2F1 (5′-TCTGGTTTTCCTTGGGTGCC-3′) and hG2R1 (5′-AGATCCTCAGCACTTTCG-3′); for the nested PCR (182 bp): hG2F2 (5′-GGTTTTCCTTGGGTGCCTTTAT-3′) and hG2R2 (5′-ATCCTCAGCACTTTCGATGG-3′). We confirmed that these primer pairs were situated in two distinct exons with an intron between them and did not amplify products originating from other GluR subunits (data not shown). PCR amplification for rat GluR2 was initiated with a denaturation step that was carried out at 95 °C for 2 min, followed by 40 cycles of 95 °C for 30 s, 62 °C for 30 s, and 72 °C for 1 min. PCR amplification for human GluR2 began with a 1 min denaturation step at 95 °C, followed by 35 cycles of denaturation at 95 °C for 10 s, annealing at 64 °C for 30 s and extension at 68 °C for 60 s. Nested PCR was conducted on 2 μl of the first PCR product under the same conditions with the exception of the annealing temperature (66 °C).

3. Results

The number of motor neurons was severely decreased in the spinal cord of SBMA patients, and we analyzed 44 neurons dissected from three cases (12 from case 1, 16 from cases 2 and 3). Restriction digestion of the PCR products yielded only 116 and 66 bp fragments but no 81 or 35 bp fragments as seen in ALS motor neurons in all the SBMA motor neurons examined. Likewise, restriction digestion of the PCR products from motor

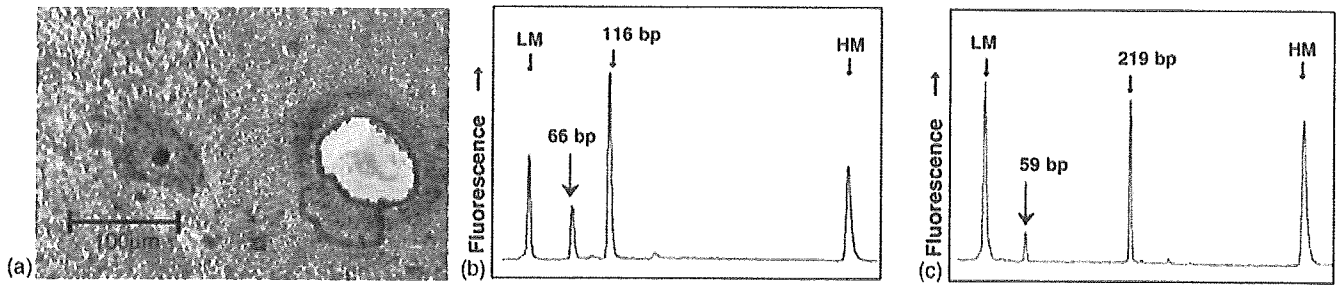

Fig. 1. (a) A single motor neuron from an SBMA patient before (left) and after (right) the dissection with a laser-microdissector. (b and c) An example of electropherogram by a 2100 Bioanalyser. Samples are the Bbv-1-digest of PCR product from tissues of a single motor neuron from an SBMA patient (b) and from a mutated human $SOD1^{G93A}$ transgenic mouse (c). LM: lower marker (15 bp), HM: higher marker (600 bp).

neurons of mutated human SOD1 transgenic rats yielded only 219 and 59 bp fragments (Fig. 1). Therefore, the values of RNA editing efficiency at the Q/R site of GluR2 were 100% in 44 motor neurons from three SBMA cases (Table 1), 55 single motor neurons from three $SOD1^{G93A}$ transgenic rats, 62 neurons from three $SOD1^{H46R}$ transgenic rats, as well as in 42 neurons from three littermate rats of each group (Table 2). The consistent finding that the GluR2 Q/R site is 100% edited in motor neurons of SBMA patients and transgenic rats for mutated human SOD1 is in marked contrast to the finding in ALS motor neurons that the editing efficiency widely varied among neurons ranging from 0% to 100% (Kawahara et al., 2004).

4. Discussion

Compared to the significant underediting reported for the GluR2 Q/R site in motor neurons of sporadic ALS (Kawahara et al., 2004), GluR2 mRNA in all the examined motor neurons of the mutated human SOD1 transgenic rats with two different mutation sites and SBMA patients was completely edited at the Q/R site. We have confirmed that postmortem delay hardly influenced the editing efficiency at the GluR2 Q/R site (Kawahara et al., 2003b), hence the significant difference in the postmortem delay between the SBMA patients in this study and ALS patients in the previous report (Kawahara et al., 2004) would not have affected these results. We examined the motor neurons in the spinal cord segment corresponding to the hindlimb of mutated human SOD1 transgenic rats after their hindlimbs had become weak, indicating that the motor neurons examined were already pathologically affected. Likewise, we found that only a small number of motor neurons remained in the spinal cord of SBMA patients. Thus our results indicate that GluR2 RNA editing was complete in the dying motor neurons in both the mutated human SOD1 transgenic rats and SBMA patients, implying that the neuronal death mechanism is not due to the underediting of GluR2 mRNA seen in sporadic ALS. Since the pathogenic mechanism underlying ALS1 is considered to be the same as in mutant human SOD1 transgenic animals, motor neurons in affected ALS1 patients would be expected to have only edited GluR2 mRNA. Indeed, an association study of the SOD1 gene in a considerable number of patients with sporadic ALS reported no significant association with mutations of the SOD1 gene (Jackson et al., 1997). Due to the lack of appropriate animal model for sporadic ALS, mutant human SOD1 transgenic animals have been used as a model for ALS in general, particularly in studies searching for therapeutically effective drugs. However, it should be kept in mind that mutated human SOD1 transgenic animals are merely a suggestive model for sporadic ALS and a gain of toxic function in mutated SOD1 kills motor neurons via mechanisms other than the demise of RNA editing. There are likely multiple different death pathways in motor neurons, and motor neurons in sporadic ALS, ALS1 and SBMA die by different death cascades.

Acknowledgements

This investigation was supported in part by grants-in-aid for Scientific Research on Priority Areas from the Ministry of Education, Culture, Sports, Science and Technology of Japan and grants from the Ministry of Health, Labor and Welfare of Japan (to SK), and a grant from Japan ALS Association (to YK).

References

Brusa, R., Zimmermann, F., Koh, D., Feldmeyer, D., Gass, P., Seeburg, P., Sprengel, R., 1995. Early-onset epilepsy and postnatal lethality associated with an editing-deficient GluR-B allele in mice. Science 270, 1677–1680.

Burnashev, N., Monyer, H., Seeburg, P., Sakmann, B., 1992. Divalent ion permeability of AMPA receptor channels is dominated by the edited form of a single subunit. Neuron 8, 189–198.

Hume, R.I., Dingledine, R., Heinemann, S.F., 1991. Identification of a site in glutamate receptor subunits that controls calcium permeability. Science 253, 1028–1031.

Jackson, M., Al-Chalabi, A., Enayat, Z.E., Chioza, B., Leigh, P.N., Morrison, K.E., 1997. Copper/zinc superoxide dismutase 1 and sporadic amyotrophic lateral sclerosis: analysis of 155 cases and identification of a novel insertion mutation. Ann. Neurol. 42, 803–807.

Katsuno, M., Adachi, H., Doyu, M., Minamiyama, M., Sang, C., Kobayashi, Y., Inukai, A., Sobue, G., 2003. Leuprorelin rescues polyglutamine-dependent phenotypes in a transgenic mouse model of spinal and bulbar muscular atrophy. Nat. Med. 9, 768–773.

Katsuno, M., Adachi, H., Kume, A., Li, M., Nakagomi, Y., Niwa, H., Sang, C., Kobayashi, Y., Doyu, M., Sobue, G., 2002. Testosterone reduction prevents phenotypic expression in a transgenic mouse model of spinal and bulbar muscular atrophy. Neuron 35, 843–854.

Kawahara, Y., Ito, K., Sun, H., Aizawa, H., Kanazawa, I., Kwak, S., 2004. RNA editing and death of motor neurons. Nature 427, 801.

Kawahara, Y., Ito, K., Sun, H., Kanazawa, I., Kwak, S., 2003a. Low editing efficiency of GluR2 mRNA is associated with a low relative abundance of

ADAR2 mRNA in white matter of normal human brain. Eur. J. Neurosci. 18, 23–33.

Kawahara, Y., Kwak, S., Sun, H., Ito, K., Hashida, H., Aizawa, H., Jeong, S.-Y., Kanazawa, I., 2003b. Human spinal motoneurons express low relative abundance of GluR2 mRNA: an implication for excitotoxicity in ALS. J. Neurochem. 85, 680–689.

Kuner, R., Groom, A.J., Bresink, I., Kornau, H.C., Stefovska, V., Muller, G., Hartmann, B., Tschauner, K., Waibel, S., Ludolph, A.C., Ikonomidou, C., Seeburg, P.H., Turski, L., 2005. Late-onset motoneuron disease caused by a functionally modified AMPA receptor subunit. Proc. Natl. Acad. Sci. U.S.A. 102, 5826–5831.

Kwak, S., Kawahara, Y., 2005. Deficient RNA editing of GluR2 and neuronal death in amyotropic lateral sclerosis. J. Mol. Med. 83, 110–120.

La Spada, A.R., Wilson, E.M., Lubahn, D.B., Harding, A.E., Fischbeck, K.H., 1991. Androgen receptor gene mutations in X-linked spinal and bulbar muscular atrophy. Nature 352, 77–79.

Nagai, M., Aoki, M., Miyoshi, I., Kato, M., Pasinelli, P., Kasai, N., Brown Jr., R.H., Itoyama, Y., 2001. Rats expressing human cytosolic copper–zinc superoxide dismutase transgenes with amyotrophic lateral sclerosis: associated mutations develop motor neuron disease. J. Neurosci. 21, 9246–9254.

Rosen, D.R., Siddique, T., Patterson, D., Figlewicz, D.A., Sapp, P., Hentati, A., Donaldson, D., Goto, J., O'Regan, J.P., Deng, H.X., et al., 1993. Mutations in Cu/Zn superoxide dismutase gene are associated with familial amyotrophic lateral sclerosis. Nature 362, 59–62.

Takuma, H., Kwak, S., Yoshizawa, T., Kanazawa, I., 1999. Reduction of GluR2 RNA editing, a molecular change that increases calcium influx through AMPA receptors, selective in the spinal ventral gray of patients with amyotrophic lateral sclerosis. Ann. Neurol. 46, 806–815.

Verdoorn, T., Burnashev, N., Monye, R.H., Seeburg, P., Sakmann, B., 1991. Structural determinants of ion flow through recombinant glutamate receptor channels. Science 252, 1715–1718.

Pharmacological induction of heat-shock proteins alleviates polyglutamine-mediated motor neuron disease

Masahisa Katsuno, Chen Sang, Hiroaki Adachi, Makoto Minamiyama, Masahiro Waza, Fumiaki Tanaka, Manabu Doyu, and Gen Sobue*

Department of Neurology, Nagoya University Graduate School of Medicine, 65 Tsurumai-cho, Showa-ku, Nagoya 466-8550, Japan

Edited by L. L. Iversen, University of Oxford, Oxford, United Kingdom, and approved September 29, 2005 (received for review July 22, 2005)

Spinal and bulbar muscular atrophy (SBMA) is an adult-onset motor neuron disease caused by the expansion of a trinucleotide CAG repeat encoding the polyglutamine tract in the first exon of the androgen receptor gene (*AR*). The pathogenic, polyglutamine-expanded AR protein accumulates in the cell nucleus in a ligand-dependent manner and inhibits transcription by interfering with transcriptional factors and coactivators. Heat-shock proteins (HSPs) are stress-induced chaperones that facilitate the refolding and, thus, the degradation of abnormal proteins. Geranylgeranylacetone (GGA), a nontoxic antiulcer drug, has been shown to potently induce HSP expression in various tissues, including the central nervous system. In a cell model of SBMA, GGA increased the levels of Hsp70, Hsp90, and Hsp105 and inhibited cell death and the accumulation of pathogenic AR. Oral administration of GGA also up-regulated the expression of HSPs in the central nervous system of SBMA-transgenic mice and suppressed nuclear accumulation of the pathogenic AR protein, resulting in amelioration of polyglutamine-dependent neuromuscular phenotypes. These observations suggest that, although a high dose appears to be needed for clinical effects, oral GGA administration is a safe and promising therapeutic candidate for polyglutamine-mediated neurodegenerative diseases, including SBMA.

spinal and bulbar muscular atrophy | geranylgeranylacetone | androgen receptor | heat-shock factor-1

Expansion of a trinucleotide CAG repeat encoding the polyglutamine tract causes inherited neurodegenerative disorders, including spinal and bulbar muscular atrophy (SBMA), Huntington's disease, dentatorubral pallidoluysian atrophy, and several forms of spinocerebellar ataxia (1, 2). All these polyglutamine diseases show progressive and refractory neurological symptoms with selective neuronal cell loss within the susceptive regions of the nervous system. SBMA is a lower motor neuron disease exclusively affecting males and characterized by adult-onset proximal muscle atrophy, weakness, fasciculations, and bulbar involvement (3, 4). The molecular basis of this disease is elongation of a polyglutamine tract in the androgen receptor (AR) protein (5), the toxicity of which is considered a major cause of neurodegeneration in SBMA (6, 7). It has been postulated that pathogenesis in SBMA results from testosterone-dependent accumulation of pathogenic, polyglutamine-expanded AR in the cell nucleus (8, 9). This hypothesis is strongly supported by the observation that intranuclear accumulation of disease-causing protein leads to transcriptional dysregulation, a supposed pathway of neurodegeneration in polyglutamine diseases (10, 11).

Accumulated polyglutamine-containing protein is commonly seen as diffuse nuclear staining or as inclusion bodies, the histopathological hallmarks of polyglutamine diseases. Although inclusion bodies appear to represent a cellular defensive response, diffusely accumulated polyglutamine-containing protein in the nucleus possesses a distinctly toxic property (12–14). Accumulation of pathogenic protein is, thus, a major target of therapeutic strategies for polyglutamine diseases. This view is supported by animal studies showing that hormonal interventions lowering serum testosterone levels successfully prevents nuclear accumulation of pathogenic AR and, thereby, rescue the phenotypes of mouse models of SBMA (8, 15, 16).

Heat-shock proteins (HSPs) are stress-induced molecular chaperones that play a crucial role in maintaining correct folding, assembly, and intracellular transport of proteins (17, 18). Under toxic conditions, HSP synthesis is rapidly up-regulated and nonnative proteins are refolded. There is increasing evidence that HSPs abrogate polyglutamine toxicity by refolding and solubilizing pathogenic proteins (19–21). Overexpression of Hsp70, together with Hsp40, inhibits toxic accumulation of abnormal polyglutamine protein and suppresses cell death in a variety of cellular models of polyglutamine diseases including SBMA (22–24). Hsp70 has also been shown to facilitate proteasomal degradation of abnormal AR protein in a cell culture model of SBMA (25). The salutary effects of Hsp70 have been verified in studies by using mouse models of polyglutamine diseases (26, 27). However, clinical applications based on these studies have certain limitations because they used genetic overexpression of Hsp70.

Geranylgeranylacetone (GGA) is an acyclic isoprenoid compound with a retinoid skeleton that induces HSP synthesis in various tissues including the gastric mucosa, intestine, liver, myocardium, retina, and central nervous system (28–32). Oral administration of GGA rapidly up-regulates HSP expression in response to a variety of stresses, although this effect is weak under nonstress conditions (29). With an extremely low toxicity, this compound has been widely used as an oral antiulcer drug. The aim of the present study is to investigate whether oral GGA induces HSP expression and thereby suppresses polyglutamine toxicity in cell culture and mouse models of SBMA.

Materials and Methods

Adenovirus Vector. Adenovirus vectors were constructed with the BD Adeno-X Expression system according to the manufacturer's protocol (Invitrogen). Briefly, truncated AR constructs containing GFP (24 CAG repeats, 215 N-terminal amino acids of AR or 97 CAG repeats, and 442 N-terminal amino acids of AR) (23) were cloned into the pShuttle vector between the NheI and XbaI sites. pShuttle vectors with truncated AR24 or AR97 were digested with I-CeuI and PI-SceI. After *in vitro* ligation, recombinant adenovirus vector constructs containing the respective transgenic fragments were used to transfect HEK293 cells, and the vectors were isolated

Conflict of interest statement: No conflicts declared.

This paper was submitted directly (Track II) to the PNAS office.

Freely available online through the PNAS open access option.

Abbreviations: SBMA, spinal and bulbar muscular atrophy; AR, androgen receptor; GGA, geranylgeranylacetone; HSP, heat-shock protein; HSF-1, heat-shock factor-1.

*To whom correspondence should be addressed. E-mail: sobueg@med.nagoya-u.ac.jp.

by using the freeze–thaw method. Finally, virus titer was determined by using the BD Adeno-X Rapid Titer kit (Invitrogen).

Cell Culture. The human neuroblastoma cell line (SH-SY5Y, American Type Culture Collection No. CRL-2266) was maintained with DMEM/F12 (Invitrogen) supplemented with 10% FCS. After neural differentiation in differentiation medium (DMEM/F12 supplemented with 5% FCS and 10 μM retinoic acid) for 4 days, SH-SY5Y cells were infected with the recombinant adenovirus vectors containing truncated AR24 or AR97 at a multiplicity of infection of 20 for 1 h and then treated with GGA. At each time point (0, 2, 4, and 6 days) after infection, cells were fixed with 4% paraformaldehyde for 10 min at room temperature, counterstained with propidium iodide (Molecular Probes), and mounted in Gelvatol. A confocal laser scanning microscope (MRC1024, Bio-Rad) and a conventional fluorescent microscope were used to determine the degree of neuronal cell death and the presence of GFP-labeled AR24 or AR97 protein in diffuse nuclear aggregates or in inclusion bodies. Quantitative analyses were made from triplicate determinations. Duplicate slides were graded blindly in two independent trials as described in ref. 23.

Immunocytochemistry. Cells were fixed with 4% paraformaldehyde and incubated with an anti-HSF-1 (HSF-1, heat-shock factor-1) antibody (1:5,000, Stressgen, Victoria, Canada) and anti-rabbit Alexa Fluor 568 antibody (1:1,000, Molecular Probes), then counterstained with Hoechst 33342 (Molecular Probes).

Animals. AR-24Q and AR-97Q mice were generated by using the pCAGGS vector as described in 8 and 33. The mouse rotarod task was performed with an Economex rotarod (Colombus Instruments, Columbus, OH), and cage activity was measured with the AB system (Neuroscience, Tokyo) as described in ref. 34. Each cage contained three mice, which were subjected to a 12-h light/dark cycle. All animal experiments were approved by the Animal Care Committee of Nagoya University Graduate School of Medicine.

GGA Treatment. GGA was a gift from Eisai, Inc. (Tokyo). For treating cultured SH-SY5Y cells, GGA was dissolved in absolute ethanol supplemented with 0.2% α-tocopherol, and ethanol with α-tocopherol alone was used as vehicle. For oral administration to mice, GGA granules were mixed with powdered rodent chow at concentrations of 0.25%, 0.5%, 1%, and 2%. GGA was administrated to mice from 6 weeks of age until the end of the analysis without withdrawal or dose reduction. All mice had unlimited access to food and water. Net consumption of GGA was determined based on the amount of food consumed in each cage.

Western Blotting. SH-SY5Y cells were lysed in CellLytic lysis buffer (Sigma–Aldrich) containing a protease inhibitor mixture (Roche Diagnostics). Mouse tissues were homogenized in buffer containing 50 mM Tris (pH 8.0), 150 mM NaCl, 1% Nonidet P-40, 0.5% deoxycholate, 0.1% SDS, and 1 mM 2-mercaptoethanol with 1 mM PMSF, and 6 μg/ml aprotinine and then centrifuged at 2,500 $\times$ g for 15 min. To extract the nuclear and cytoplasmic fractions, mouse tissues were treated with NE-PER nuclear and cytoplasmic extraction reagents (Pierce); cultured cells were lysed in buffer containing 10 mM Tris·HCl (pH 7.4), 10 mM NaCl, 3 mM MgCl2, and 0.5% Nonidet P-40 and then suspended in buffer containing 50 mM Tris·HCl (pH 6.8), 2% SDS, 6% glycerol, and protease inhibitor mixture (Roche Diagnostics). Equal amounts of protein were separated by 5–20% SDS/PAGE and transferred to Hybond-P membranes (Amersham Pharmacia Biotech). Primary antibodies and concentrations were as follows: AR (H-280, 1:1,000, Santa Cruz Biotechnology) Hsp70 (1:1,000, Stressgen Biotechnologies, Victoria, Canada), Hsc70 (1:5,000, Stressgen Biotechnologies), Hsp25 (1:5,000, Stressgen Biotechnologies), Hsp40 (1:5,000, Stressgen Biotechnologies), Hsp60 (1:5,000, Stressgen Biotechnologies), Grp78 (1:5,000, Stressgen Biotechnologies), Hsp90 (1:1,000, Stressgen Biotechnologies), Hsp105 (1:250, Novocastra Laboratories, Newcastle, U.K.), HSF-1 (1:5,000, Stressgen Biotechnologies), and thioredoxin (1:2,000, Redox Bioscience, Kyoto, Japan). Primary antibody binding was probed with horseradish peroxidase-conjugated secondary antibodies at a dilution of 1:5,000, and bands were detected by using immunoreaction enhance solution (Can Get Signal, Toyobo, Japan) and enhanced chemiluminescence (ECL Plus, Amersham Biosciences, which is now GE Healthcare). An LAS-3000 imaging system (Fuji) was used to produce digital images. Signal intensities of three independent blots were quantified with IMAGE GAUGE software version 4.22 (Fuji) and expressed in arbitrary units. Membranes were reprobed with anti-α-tubulin (1:5,000, Santa Cruz Biotechnology), or anti-histone H3 (1:500, Upstate Biotechnology, Lake Placid, NY) antibodies for normalization.

Immunohistochemistry. Mice anesthetized with ketamine-xylazine were perfused with 4% paraformaldehyde fixative in phosphate buffer (pH 7.4). Tissues were dissected, postfixed in 10% phosphate-buffered formalin, and processed for paraffin embedding. Sections to be stained with anti-polyglutamine antibody *1C2* were treated with formic acid for 5 min at room temperature; those to be incubated with anti-HSF-1 antibody were boiled in 10 mM citrate buffer for 15 min. Primary antibodies and dilutions were as follows: polyglutamine (1:20,000, Chemicon, Temecula, CA), Hsp70 (1:500, Stressgen Biotechnologies), and anti-HSF-1 (1:5000, Stressgen Biotechnologies). Primary antibody binding was probed with a labeled polymer of secondary antibody as part of the Envision+ system containing horseradish peroxidase (DakoCytomation, Gostrup, Denmark). The number of 1C2-positive cells in the spinal cord and muscle were determined as described in ref. 27.

Statistical Analyses. We analyzed data by using the Kaplan–Meier and log-rank test for survival rate, ANOVA with Dunnett's post hoc test for multiple comparisons, and an unpaired t test from STATVIEW software version 5 (Hulinks, Tokyo).

Results

GGA Suppresses Polyglutamine Toxicity in Cellular Model of SBMA. To test whether GGA suppresses cellular toxicity induced by expanded polyglutamine, we generated a cultured cell model of SBMA. Adenovirus vector-mediated expression of a truncated AR with 97 CAGs (tAR97Q) resulted in the formation of inclusion bodies in the nucleus and cytoplasm as well as eventual cell death in human neuroblastoma cell line SH-SY5Y, whereas expression of AR containing only 24 CAGs (tAR24Q) showed no such toxicity (Fig. 1 *A* and *B*). GGA administration reduced neuronal cell death as detected by propidium iodide staining in the cells expressing tAR97Q, the strongest effect occurring at a dose of 10^{-9} M (Fig. 1 *B* and *C*). Although GGA failed to decrease the number of the cells containing inclusion bodies, Western blot analysis using an anti-AR N terminus antibody demonstrated that GGA significantly diminished the amount of a high-molecular-weight complex, which likely corresponds to oligomers of tAR97Q (Fig. 1 *D* and *E*) (35). Thus, GGA treatment suppresses cytotoxicity caused by accumulation of AR with elongated polyglutamine without inhibiting inclusion body formation.

GGA Induces HSPs in Cellular Model of SBMA. To determine whether the GGA-mediated mitigation of polyglutamine toxicity is due to HSP expression, we determined HSP levels in the cell culture model of SBMA after GGA treatment. GGA up-regulated expression of Hsp70, Hsp90, and Hsp105 in the cells with tAR97Q but did not in those with tAR24Q (Fig. 2 *A* and *B*). Cycloheximide treatment eliminated GGA-mediated HSP induction and suppression of cell death (Fig. 2 *C* and *D*). Expression of Hsc70, a constitutively expressed HSP, was not increased by GGA treatment; no GGA-mediated up-regulation was detected for other HSPs tested, such as

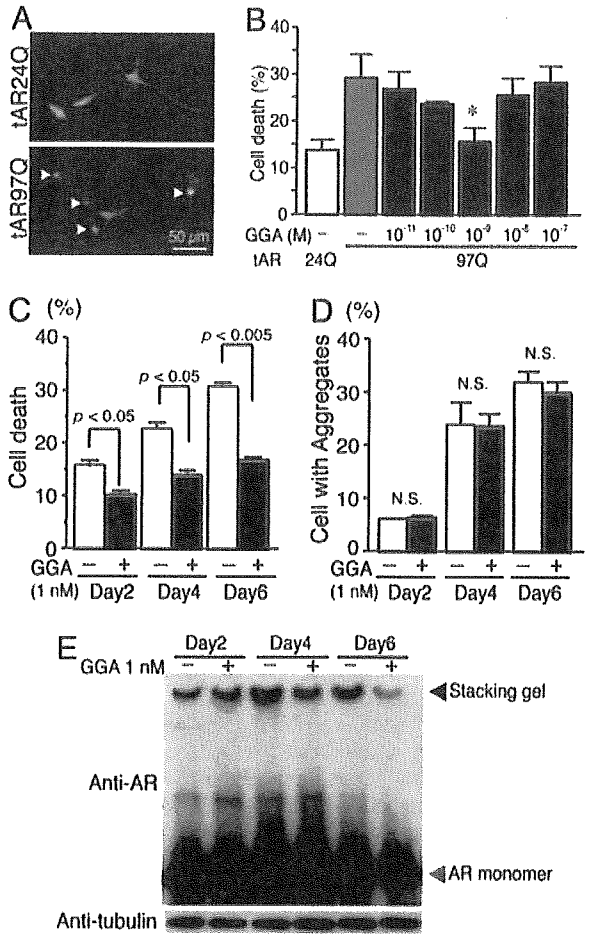

Fig. 1. Effects of GGA on polyglutamine toxicity in cultured cell. (*A*) Punctuated aggregates visualized with GFP (arrowhead) are formed in SHSY-5Y cells infected with an adenovirus vector containing truncated AR with 97 CAGs (tAR97Q-GFP) but not in those bearing tAR24Q. (*B*) Frequency of cell death 6 days after infection as detected by propidium iodine staining (*, $P < 0.05$ compared with untreated tAR97Q cells). (*C*) Suppression of cell death by GGA. (*D*) Frequency of cells bearing aggregates. (*E*) Anti-AR analysis of Western blots of extracts from cells infected with tAR97Q. Error bars indicate SD.

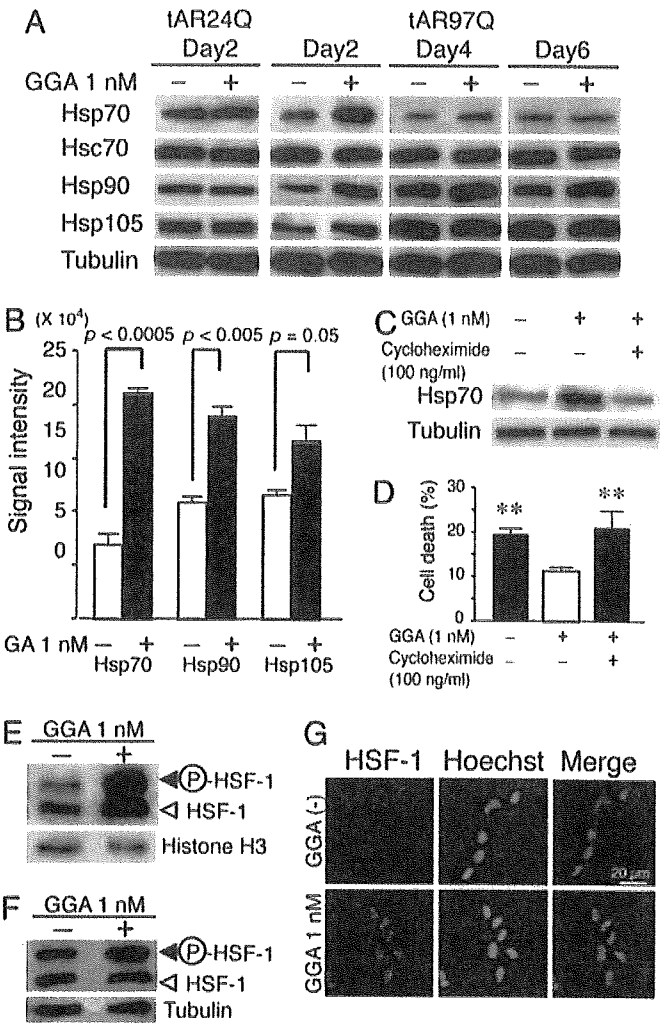

Fig. 2. GGA-mediated HSP induction in cultured cell. (*A*) Anti-HSP analysis of Western blots from cells infected with tAR97Q and treated with GGA. (*B*) Quantification of the levels of HSPs from tAR97Q-infected cells after 2 days of GGA treatment. (*C*) Anti-Hsp70 analysis of Western blots from tAR97Q cells treated with or without cycloheximide. (*D*) Frequency of cell death 2 days after infection as detected by propidium iodine staining (**, $P < 0.05$ compared with tAR97Q cells treated with GGA but not with cycloheximide). (*E* and *F*) Anti-HSF-1 analysis of Western blots of the cellular nuclear fraction (*E*) and that of total cell lysate (*F*). Upper bands correspond to the hyperphosphorylated, active form of HSF-1. (*G*) Immunocytochemistry for HSF-1. Error bars indicate SD.

Hsp40 and Hsp60, or for thioredoxin, a redox-regulating protein (data not shown). Western blotting (Fig. 2 *E* and *F*) and immunocytochemistry (Fig. 2*G*) revealed that GGA increased the nuclear uptake of hyperphosphorylated HSF-1, a transcription factor regulating HSP expression in the nucleus. Given that activated HSF-1 forms a hyperphosphorylated trimer and translocates into the nucleus, these findings suggest that GGA activates HSF-1, leading to HSP up-regulation.

GGA Ameliorates Symptomatic Phenotypes of SBMA Mouse. To examine whether pharmacological induction of HSPs alleviates polyglutamine-dependent neuronal dysfunction, oral GGA was administrated to transgenic mice bearing human AR with 97 CAGs (AR-97Q). The actual amount of GGA was constant in each treatment group during the treatment period (see Table 1, which is published as supporting information on the PNAS web site). Oral GGA ameliorated muscle atrophy, gait disturbance, rotarod disability, and body weight loss in AR-97Q mice at both doses of 0.5 and 1% of food, which correspond to ≈600 and 1,200 $mg \cdot kg^{-1} \cdot day^{-1}$, respectively (Fig. 3 *A–E* and Table 1). The life span of AR-97Q mice treated orally with 0.5 or 1% GGA was significantly extended compared with that of untreated AR-97Q mice. ($P < 0.001$) (Fig. 3*F*). GGA failed to alleviate motor dysfunction in AR-97Q mice at a dose of 0.25%. A higher dose of GGA, 2% of food, inhibited body growth and had no beneficial effects on the neurological phenotypes of the AR-97Q mice. Although no hepatic or renal toxicity was demonstrated at other doses, this high dose caused liver enlargement and dysfunction in wild-type and transgenic mice (see Table 2, which is published as supporting information on the PNAS web site).

GGA Induces HSP Expression in SBMA Mice Through HSF-1 Activation. To examine whether the GGA-induced improvement in the phenotypes of AR-97Q mice was due to induction of HSPs, the expression levels of HSPs were determined. Oral GGA increased the expression of Hsp70, Hsp90, and Hsp105 in the central nervous system and in the skeletal muscle of AR-97Q mice at the doses (0.5 and 1% of food) that were shown to improve symptomatic phenotypes of AR-97Q mice (Fig. 4 *A–C* and Fig. 6 *A* and *B*, which is published as supporting information on the PNAS web site). The

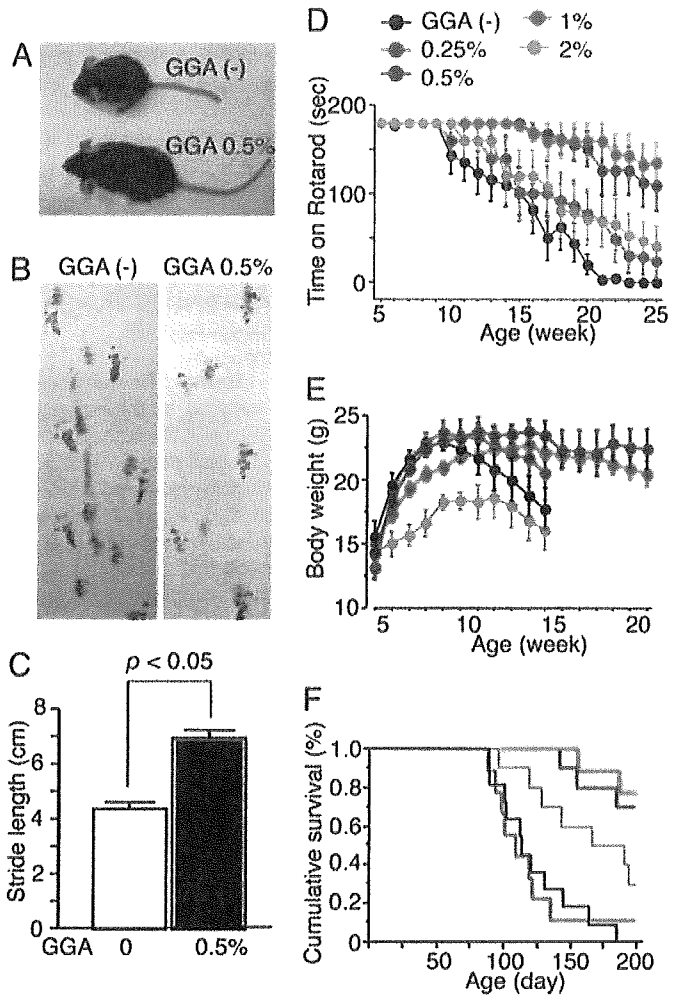

Fig. 3. Effect of GGA on neurological phenotypes of AR-97Q mice. (*A*) Muscle atrophy of 13-week AR-97Q mice. (*B*) Footprints of 13-week AR-97Q mice. Front paws are shown in red, and hind paws are shown in blue. (*C*) Stride distance of 13-week AR-97Q mice ($n = 3$ for each group). (*D–F*) Rotarod task (*D*), body weight (*E*), and cumulative survival (*F*) of male AR-97Q mice treated with GGA ($n = 12$ for each group) and untreated counterparts ($n = 15$). Rotarod performance significantly improved after GGA at doses of 0.5% and 1.0% ($P < 0.0001$ at both doses compared with nontreated mice at 20 weeks), and body weight increased significantly at a dose of 0.5% ($P < 0.005$ at 0.5% and $P < 0.05$ at 1.0%, at 14 weeks). Error bars indicate SD.

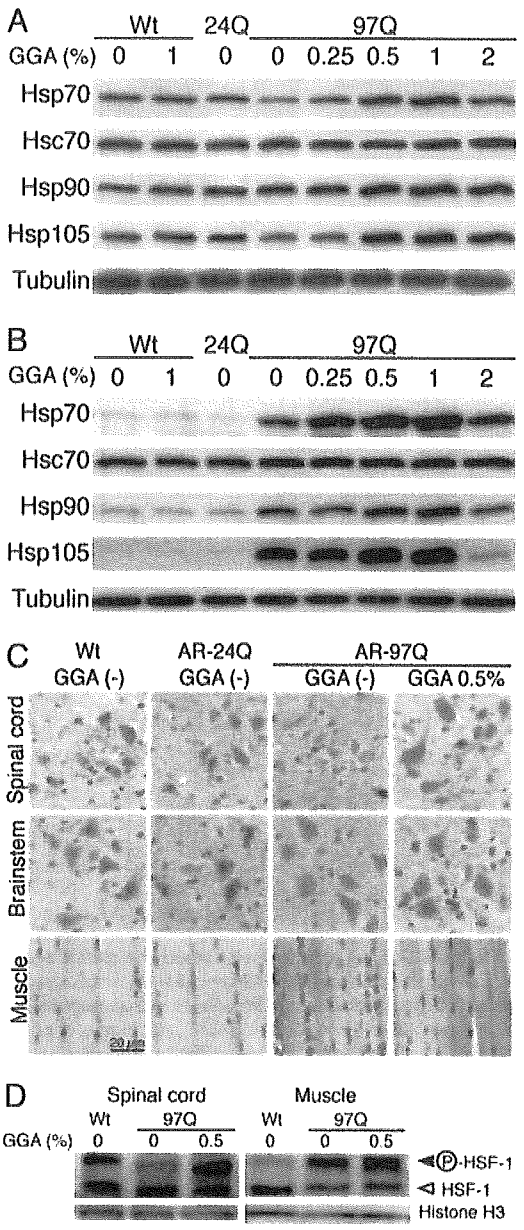

Fig. 4. GGA-mediated HSP induction in AR-97Q mice. (*A*) Western blotting for various HSPs in the spinal cord of 14-week, wild-type (Wt), AR-24Q and AR-97Q mice. (*B*) Western blotting for various HSPs in skeletal muscle of 14-week wild-type, AR-24Q, and AR-97Q mice. (*C*) Immunohistochemistry for Hsp70 in 14-week wild-type, AR-24Q, and AR-97Q mice. (*D*) Western blotting of nuclear fraction from spinal cord and that from muscle using anti-HSF-1 antibody. Upper bands correspond to the hyperphosphorylated active form of HSF-1.

induction of HSPs was not clearly observed in the central nervous system until 3 weeks after treatment initiation, but it continued for at least 4 weeks thereafter (see Fig. 7*A*, which is published as supporting information on the PNAS web site). HSP induction by GGA was undetectable at a dose of 0.25% and was not significant at 2%, in agreement with the lack of therapeutic effect on motor function at these doses. Grp78, Hsp25, Hsp40, Hsp60, and thioredoxin were not induced by GGA administration (see Fig. 7*B*).

To examine whether GGA induced HSP expression through HSF-1 activation, the nuclear translocation of HSF-1 was investigated after GGA treatment. In the untreated state, the level of nuclear accumulated hyperphosphorylated HSF-1 in the central nervous systems of AR-97Q mice was lower than in the wild-type mice. However, when AR-97Q mice received 0.5% oral GGA, nuclear translocation of HSF-1 was higher than in the nontreated mice (Fig. 4*D* and Fig. 8, which is published as supporting information on the PNAS web site). In contrast, nuclear translocation of HSF-1 in skeletal muscle of untreated AR-97Q mice is already much higher than in wild-type mice, thus perhaps explaining the high degree of Hsp70 induction in AR-97Q mice. After GGA treatment, nuclear translocation of HSF-1 in skeletal muscle of AR-97Q mice was even higher than it was in untreated AR-97Q mice, contributing to a higher induction of Hsp70 (Figs. 4*D* and 8). These experiments suggest that oral GGA restores activation of HSF-1, which is inhibited by expanded polyglutamine in the affected nervous tissues of AR-97Q mice.

GGA Inhibits Accumulation of Pathogenic AR in Nucleus. With the aim of evaluating the effect of GGA on the nuclear accumulation of abnormal AR, immunohistochemistry with anti-polyglutamine an-

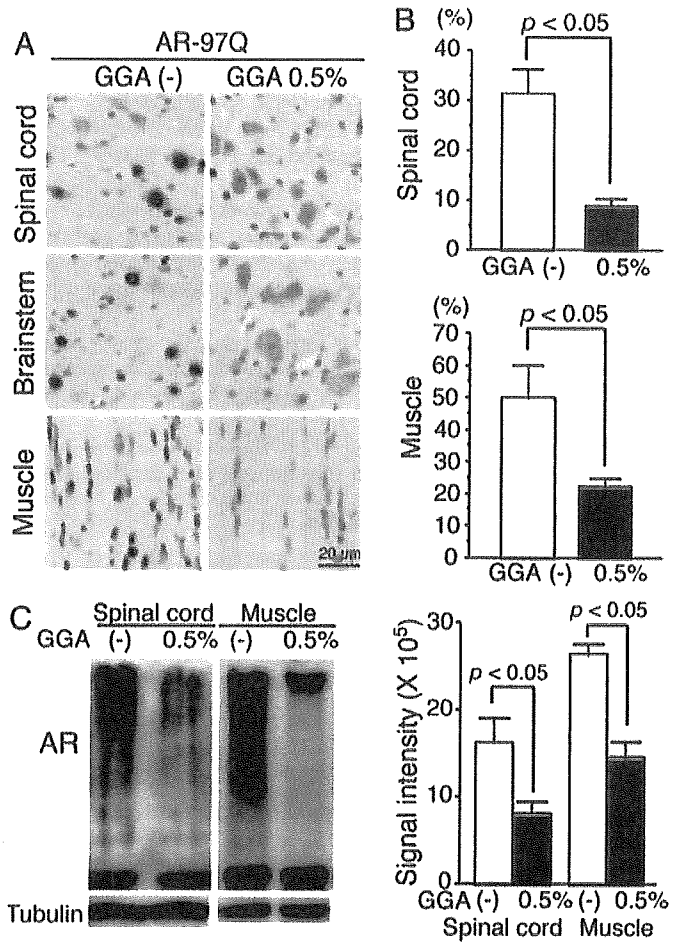

Fig. 5. Effect of GGA on accumulation of abnormal AR. (*A*) Immunohistochemistry of 14-week wild-type, AR-24Q, and AR-97Q mice using 1C2 antibody. (*B*) Quantification of 1C2-positive cells in spinal cord and muscle of AR-97Q mice treated with or without GGA. (*C*) Western blotting for AR of 14-week AR-97Q mice and quantification of the high-molecular-weight, abnormal AR complex indicated by a smear from the top of the gel. Error bars indicate SD.

tibody 1C2 was performed on tissues from GGA-administrated and untreated AR-97Q mice. Oral 0.5% GGA decreased the number of 1C2-positive cells in nervous tissues and, to a lesser extent, in muscle (Fig. 5 *A* and *B*). Western blot analysis using an antibody against AR demonstrated that 0.5% oral GGA reduced the amount of the high-molecular-weight complex of abnormal AR (Fig. 5*C*). These findings suggest that oral GGA-mediated HSP induction inhibits nuclear accumulation of abnormal AR, leading to mitigation of polyglutamine-dependent pathogenesis.

Discussion

GGA Induces HSP Expression. In the present study, GGA induced Hsp70, Hsp90, and Hsp105 in a cultured cell model of SBMA, leading to abrogation of polyglutamine-mediated cytotoxicity. Furthermore, oral GGA alleviated neuronal dysfunction through induction of HSPs in SBMA mice.

GGA was first introduced as a nontoxic inducer of Hsp70 in rat gastric mucosa (28). Oral GGA has also been reported to induce Hsp70 in the central nervous system as well as in the small intestine, liver, heart, and retina of rodents without any adverse effects (29–32, 36, 37). The present study suggests that the required dose for HSP induction in the SBMA mouse model is ≈600 $mg \cdot kg^{-1} \cdot day^{-1}$, whereas 200 $mg \cdot kg^{-1} \cdot day^{-1}$ induces HSP expression in nonneuronal tissues of rodents under stress (28, 36). Several studies have verified that Hsp70 induction is due to GGA-mediated activation of HSF-1, a transcription factor that regulates expression of Hsp70 (28, 37). In the SBMA mice, GGA facilitated nuclear translocation of HSF-1, leading to induction of Hsp70, in the affected tissues.

GGA showed no adverse effects at the salutary doses used in the present study, although hepatic toxicity was detected at a higher dose. Low toxicity of GGA is advantageous, because continuous administration of GGA at a high dose is required for treating slowly progressive neurodegenerative disease (6, 7). Pharmacological induction of HSP by using GGA thus appears to be an applicable therapeutic strategy for SBMA, although careful attention should be paid to adverse effects during long-term treatment.

HSPs as Therapeutics for Polyglutamine Diseases. In the present study, GGA-mediated HSP induction resulted in inhibiting the accumulation of abnormal AR in the cellular and transgenic mouse models of SBMA. Accumulation of abnormal protein has been considered central to the pathogenesis of polyglutamine diseases, including SBMA. It has been postulated that expanded polyglutamine confers a monomeric protein conformational change from random coil to β-sheet, leading to formation of a polyglutamine oligomer (38, 39). The misfolded monomer and oligomer exercise their toxic effects by interacting with normal cellular proteins. Direct inhibition of polyglutamine oligomerization by Congo red has been demonstrated to exert therapeutic effects in a mouse model of Huntington's disease (40). Whereas oligomerization of causative proteins has been implicated in the pathogenic processes of neurodegeneration in polyglutamine diseases, the formation of inclusion bodies or mature amyloid fibrils appears to possess cytoprotective properties (13, 41). Based on this hypothesis, HSPs have been drawing a great deal of attention because they inhibit oligomer assembly and thereby mitigate polyglutamine toxicity (20, 21, 38). This view is supported by the fact that overexpression of Hsp70 attenuates the accumulation of polyglutamine-containing protein, resulting in amelioration of neurodegeneration in animal models of spinocerebellar ataxias or SBMA (26, 27).

GGA treatment significantly suppressed nuclear accumulation of abnormal AR in SBMA mice but did not inhibit inclusion body formation in cultured cells. This inconsistency does not necessarily deny a beneficial effect of GGA on polyglutamine aggregation, because it can be explained by several lines of evidence: (*i*) HSPs facilitate amyloid fibril formation by stabilizing the conformation of abnormal polyglutamine-expanded protein (42), and (*ii*) HSPs biochemically alter the structure of inclusion bodies (43, 44).

Hsp70 overexpression, however, fails to alleviate neurodegeneration or aggregate formation in the R6/2 mouse model of Huntington's disease (45, 46). This discord appears to indicate that higher levels of Hsp70 or the concomitant induction of other HSPs is required to alleviate Huntington's disease pathology. In addition to Hsp70, various molecular chaperones that colocalize with aggregates have also been shown to suppress polyglutamine toxicity: Hsp40-associated Hsp70 (23, 43), Hsp90, and Hsp105 (47, 48). Oral GGA induced Hsp90 and Hsp105 in the mouse model of SBMA and such diverse HSP up-regulation might contribute to the beneficial effects of GGA in the SBMA mice.

HSP in Pathogenesis of polyQ Diseases. Not only are HSPs considered potent suppressors of polyglutamine toxicity, but they are also implicated in the pathogenesis of neurodegeneration (20). There are several lines of evidence that polyglutamine elongation weakens the protective responses for coping with cellular stress. Truncated AR with expanded polyglutamine delays the induction of Hsp70 after heat shock (49). In the SBMA mice we examined, the level of Hsp70 in spinal cord was decreased before the onset of motor dysfunction. A similar finding has also been reported in the R6/2 mouse model of Huntington's disease (46).

In our SBMA mice, abnormal, polyglutamine-expanded AR seems to inhibit nuclear translocation of HSF-1 in the central nervous system, leading to a decrease in the level of Hsp70. In mammalian cells, induction of Hsp70 requires activation and nuclear localization of HSF-1. In the presence of nonnative protein, HSF-1 is derepressed, forming a trimer that translocates into the nucleus and binds to heat-shock elements within the gene encoding Hsp70 (50). In cellular models, this stress-induced nuclear accumulation of HSF-1 has been designated nuclear granules (51). Aggregates of abnormal ataxin-1, the causative protein in spinocerebellar ataxia 1, have been shown to hinder induction of nuclear granules in response to heat shock (52). Therefore, failure of HSF-1 activation appears to enhance polyglutamine toxicity. In this context, it is intriguing that inhibition of the nuclear accumulation of HSF-1 was detected in spinal cord but not in muscle of SBMA transgenic mice. Given that the threshold for HSP induction is relatively high in motor neurons (53), motor-neuron-specific inactivation of HSP transcription might partially explain why the central nervous system is selectively affected in polyglutamine diseases including SBMA.

HSP-Based Therapy for Neurodegeneration. Both genetic and pharmacological manipulations of HSPs have been demonstrated to mitigate the pathogenesis of neurodegeneration (54–57). These observations suggest that GGA-mediated HSP induction may provide a therapeutic strategy for diverse neurodegenerative disorders, because these diseases share common pathogenic mechanisms such as abnormal protein aggregation, disruption of the ubiquitin-proteasome system and activation of the apoptotic pathway.

In summary, our observations indicate that GGA is a safe and promising therapeutic approach for treating many devastating neurodegenerative diseases, including SBMA.

We thank Eisai, Inc. for providing GGA. This work was supported by a Center-of-Excellence grant from the Ministry of Education, Culture, Sports, Science and Technology of Japan and grants from the Ministry of Health, Labor, and Welfare of Japan.

1. Zoghbi, H. Y. & Orr, H. T. (2000) *Annu. Rev. Neurosci.* **23,** 217–247.
2. Ross, C. A. (2002) *Neuron* **35,** 819–822.
3. Kennedy, W. R., Alter, M. & Sung, J. H. (1968) *Neurology* **18,** 671–680.
4. Sobue, G., Hashizume, Y., Mukai, E., Hirayama, M., Mitsuma, T. & Takahashi, A. (1989) *Brain* **112,** 209–232.
5. La Spada, A. R., Wilson, E. M., Lubahn, D. B., Harding, A. E. & Fischbeck, K. H. (1991) *Nature* **352,** 77–79.
6. Fischbeck, K. H., Lieberman, A., Bailey, C. K., Abel, A. & Merry, D. E. (1999) *Philos. Trans. R. Soc. London B* **354,** 1075–1078.
7. Katsuno, M., Adachi, H., Tanaka, F. & Sobue, G. (2004) *J. Mol. Med.* **82,** 298–307.
8. Katsuno, M., Adachi, H., Kume, A., Li, M., Nakagomi, Y., Niwa, H., Sang, C., Kobayashi, Y., Doyu, M. & Sobue, G. (2002) *Neuron* **35,** 843–854.
9. Takeyama, K., Ito, S., Yamamoto, A., Tanimoto, H., Furutani, T., Kanuka, H., Miura, M., Tabata, T. & Kato, S. (2002) *Neuron* **35,** 855–864.
10. Nucifora, F. C., Jr., Sasaki, M., Peters, M. F., Huang, H., Cooper, J. K., Yamada, M., Takahashi, H., Tsuji, S., Troncoso, J., Dawson, V. L., Dawson, T. M. & Ross, C. A. (2001) *Science* **291,** 2423–2428.
11. Minamiyama, M., Katsuno, M., Adachi, H., Waza, M., Sang, C., Kobayashi, Y., Tanaka, F., Doyu, M., Inukai, A. & Sobue, G. (2004) *Hum. Mol. Genet.* **13,** 1183–1192.
12. Yamada, M., Wood, J. D., Shimohata, T., Hayashi, S., Tsuji, S., Ross, C. A. & Takahashi, H. (2001) *Ann. Neurol.* **49,** 14–23.
13. Arrasate, M., Mitra, S., Schweitzer, E. S., Segal, M. R. & Finkbeiner, S. (2004) *Nature* **431,** 805–810.
14. Adachi, H., Katsuno, M., Minamiyama, M., Waza, M., Sang, C., Nakagomi, Y., Kobayashi, Y., Tanaka, F., Doyu, M. & Inukai, A., *et al.* (2005) *Brain* **128,** 659–670.
15. Katsuno, M., Adachi, H., Doyu, M., Minamiyama, M., Sang, C., Kobayashi, Y., Inukai, A. & Sobue, G. (2003) *Nat. Med.* **9,** 768–773.
16. Chevalier-Larsen, E. S., O'Brien, C. J., Wang, H., Jenkins, S. C., Holder, L., Lieberman, A. P. & Merry, D. E. (2004) *J. Neurosci.* **24,** 4778–4786.
17. Welch, W. J. & Brown, C. R. (1996) *Cell Stress Chaperones* **1,** 109–115.
18. Morimoto, R. I. & Santoro, M. G. (1998) *Nat. Biotechnol.* **16,** 833–838.
19. Kobayashi, Y. & Sobue, G. (2001) *Brain Res. Bull.* **56,** 165–168.
20. Wyttenbach, A. (2004) *J. Mol. Neurosci.* **23,** 69–96.
21. Muchowski, P. J. & Wacker, J. L. (2005) *Nat. Rev. Neurosci.* **6,** 11–22.
22. Cummings, C. J., Mancini, M. A., Antalffy, B., DeFranco, D. B., Orr, H. T. & Zoghbi, H. Y. (1998) *Nat. Genet.* **19,** 148–154.
23. Kobayashi, Y., Kume, A., Li, M., Doyu, M., Hata, M., Ohtsuka, K. & Sobue, G. (2000) *J. Biol. Chem.* **275,** 8772–8778.
24. Wyttenbach, A., Swartz, J., Kita, H., Thykjaer, T., Carmichael, J., Bradley, J., Brown, R., Maxwell, M., Schapira, A., Orntoft, T. F., *et al.* (2001) *Hum. Mol. Genet.* **10,** 1829–1845.
25. Bailey, C. K., Andriola, I. F., Kampinga, H. H. & Merry, D. E. (2002) *Hum. Mol. Genet.* **11,** 515–523.
26. Cummings, C. J., Sun, Y., Opal, P., Antalffy, B., Mestril, R., Orr, H. T., Dillmann, W. H. & Zoghbi, H. Y. (2001) *Hum. Mol. Genet.* **10,** 1511–1518.
27. Adachi, H., Katsuno, M., Minamiyama, M., Sang, C., Pagoulatos, G., Angelidis, C., Kusakabe, M., Yoshiki, A., Kobayashi, Y., Doyu, M. & Sobue, G. (2003) *J. Neurosci.* **23,** 2203–2211.
28. Hirakawa, T., Rokutan, K., Nikawa, T. & Kishi, K. (1996) *Gastroenterology* **111,** 345–357.
29. Yamagami, K., Yamamoto, Y., Ishikawa, Y., Yonezawa, K., Toyokuni, S. & Yamaoka, Y. (2000) *J. Lab. Clin. Med.* **135,** 465–475.
30. Ooie, T., Takahashi, N., Saikawa, T., Nawata, T., Arikawa, M., Yamanaka, K., Hara, M., Shimada, T. & Sakata, T. (2001) *Circulation* **104,** 1837–1843.
31. Ishii, Y., Kwong, J. M. & Caprioli, J. (2003) *Invest. Ophthalmol. Vis. Sci.* **44,** 1982–1992.
32. Fujiki, M., Kobayashi, H., Abe, T. & Ishii, K. (2003) *Brain Res.* **991,** 254–257.
33. Niwa, H., Yamamura, K. & Miyazaki, J. (1991) *Gene* **108,** 193–199.
34. Adachi, H., Kume, A., Li, M., Nakagomi, Y., Niwa, H., Do, J., Sang, C., Kobayashi, Y., Doyu, M. & Sobue, G. (2001) *Hum. Mol. Genet.* **10,** 1039–1048.
35. Iuchi, S., Hoffner, G., Verbeke, P., Djian, P. & Green, H. (2003) *Proc. Natl. Acad. Sci. USA* **100,** 2409–2414.
36. Tsuruma, T., Yagihashi, A., Koide, S., Araya, J., Tarumi, K., Watanabe, N. & Hirata, K. (1999) *Transplant Proc.* **31,** 572–573.
37. Yamanaka, K., Takahashi, N., Ooie, T., Kaneda, K., Yoshimatsu, H. & Saikawa, T. (2003) *J. Mol. Cell Cardiol.* **35,** 785–794.
38. Sakahira, H., Breuer, P., Hayer-Hartl, M. K. & Hartl, F. U. (2002) *Proc. Natl. Acad. Sci. USA* **99,** 16412–16418.
39. Perutz, M. F., Pope, B. J., Owen, D., Wanker, E. E. & Scherzinger, E. (2002) *Proc. Natl. Acad. Sci. USA* **99,** 5596–5600.
40. Sanchez, I., Mahlke, C. & Yuan, J. (2003) *Nature* **421,** 373–379.
41. Wacker, J. L., Zareie, M. H., Fong, H., Sarikaya, M. & Muchowski, P. J. (2004) *Nat. Struct. Mol. Biol.* **11,** 1215–1222.
42. Hsu, A. L., Murphy, C. T. & Kenyon, C. (2003) *Science* **300,** 1142–1145.
43. Muchowski, P. J., Schaffar, G., Sittler, A., Wanker, E. E., Hayer-Hartl, M. K. & Hartl, F. U. (2000) *Proc. Natl. Acad. Sci. USA* **97,** 7841–7846.
44. Chan, H. Y., Warrick, J. M., Gray-Board, G. L., Paulson, H. L. & Bonini, N. M. (2000) *Hum. Mol. Genet.* **9,** 2811–2820.
45. Hansson, O., Nylandsted, J., Castilho, R. F., Leist, M., Jaattela, M. & Brundin, P. (2003) *Brain Res.* **970,** 47–57.
46. Hay, D. G., Sathasivam, K., Tobaben, S., Stahl, B., Marber, M., Mestril, R., Mahal, A., Smith, D. L., Woodman, B. & Bates, G. P. (2004) *Hum. Mol. Genet.* **13,** 1389–1405.
47. Mitsui, K., Nakayama, H., Akagi, T., Nekooki, M., Ohtawa, K., Takio, K., Hashikawa, T. & Nukina, N. (2002) *J. Neurosci.* **22,** 9267–9277.
48. Ishihara, K., Yamagishi, N., Saito, Y., Adachi, H., Kobayashi, Y., Sobue, G., Ohtsuka, K. & Hatayama, T. (2003) *J. Biol. Chem.* **278,** 25143–25150.
49. Cowan, K. J., Diamond, M. I. & Welch, W. J. (2003) *Hum. Mol. Genet.* **12,** 1377–1391.
50. Santoro, M. G. (2000) *Biochem. Pharmacol.* **59,** 55–63.
51. Morimoto, R. I. (1998) *Genes Dev.* **12,** 3788–3796.
52. Rimoldi, M., Servadio, A. & Zimarino, V. (2001) *Brain Res. Bull.* **56,** 353–362.
53. Batulan, Z., Shinder, G. A., Minotti, S., He, B. P., Doroudchi, M. M., Nalbantoglu, J., Strong, M. J. & Durham, H. D. (2003) *J. Neurosci.* **23,** 5789–5798.
54. Kieran, D., Kalmar, B., Dick, J. R., Riddoch-Contreras, J., Burnstock, G. & Greensmith, L. (2004) *Nat. Med.* **10,** 402–405.
55. Auluck, P. K., Chan, H. Y., Trojanowski, J. Q., Lee, V. M. & Bonini, N. M. (2002) *Science* **295,** 865–868.
56. Kikuchi, S., Shinpo, K., Takeuchi, M., Tsuji, S., Yabe, I., Niino, M. & Tashiro, K. (2002) *J. Neurosci. Res.* **69,** 373–381.
57. Waza, M., Adachi, H., Katsuno, M., Minamiyama, M., Sang, C., Tanaka, F., Inukai, A., Doyu, M. & Sobue, G. (2005) *Nat. Med.* **11,** 1088–1095.

nature medicine

17-AAG, an Hsp90 inhibitor, ameliorates polyglutamine-mediated motor neuron degeneration

Masahiro Waza[1,2], Hiroaki Adachi[1,2], Masahisa Katsuno[1], Makoto Minamiyama[1], Chen Sang[1], Fumiaki Tanaka[1], Akira Inukai[1], Manabu Doyu[1] & Gen Sobue[1]

Heat-shock protein 90 (Hsp90) functions as part of a multichaperone complex that folds, activates and assembles its client proteins. Androgen receptor (AR), a pathogenic gene product in spinal and bulbar muscular atrophy (SBMA), is one of the Hsp90 client proteins. We examined the therapeutic effects of 17-allylamino-17-demethoxygeldanamycin (17-AAG), a potent Hsp90 inhibitor, and its ability to degrade polyglutamine-expanded mutant AR. Administration of 17-AAG markedly ameliorated motor impairments in the SBMA transgenic mouse model without detectable toxicity, by reducing amounts of monomeric and aggregated mutant AR. The mutant AR showed a higher affinity for Hsp90-p23 and preferentially formed an Hsp90 chaperone complex as compared to wild-type AR; mutant AR was preferentially degraded in the presence of 17-AAG in both cells and transgenic mice as compared to wild-type AR. 17-AAG also mildly induced Hsp70 and Hsp40. 17-AAG would thus provide a new therapeutic approach to SBMA and probably to other related neurodegenerative diseases.

Hsp90, which accounts for 1–2% of cytosolic protein, is one of the most abundant cellular chaperone proteins[1]. It functions in a multicomponent complex of chaperone proteins including Hsp70, Hop (Hsp70 and Hsp90 organizing protein), Cdc37, Hsp40 and p23. Hsp90 is involved in the folding, activation and assembly of several proteins, known as Hsp90 client proteins[1]. As numerous oncoproteins have been shown to be Hsp90 client proteins[1], Hsp90 inhibitors have become a new strategy in antitumor therapy[2]. Geldanamycin, a classical Hsp90 inhibitor, is known as a potent antitumor agent[2]; however, it has not been used in clinical trials because of its liver toxicity[3]. 17-AAG is a new derivative of geldanamycin that shares its important biological activities[4] but shows less toxicity[5].

Hsp90 requires several interacting, co-chaperone proteins to exert its function on Hsp90 client proteins in Hsp90 complexes[1], of which two main forms exist[6]. One complex is a proteasome-targeting form associated with Hsp70 and Hop, and the other is a stabilizing form with Cdc37 and p23 (refs. 7,8). Particularly, p23 is thought to modulate Hsp90 activity in the last stages of the chaperoning pathway, leading to stabilized Hsp90 client proteins[9]. Hsp90 inhibitors, including 17-AAG, inhibit the progression of the Hsp90 complex toward the stabilizing form[10–12], and shift it to the proteasome-targeting form[7,8], resulting in enhanced proteasomal degradation of the Hsp90 client protein[7,13–18].

Because 17-AAG has less toxicity and higher selectivity for client oncoproteins[19], 17-AAG is now in clinical trials for a wide range of malignancies[20]. Additionally, Hsp90 inhibitors also function as Hsp inducers[20,21]. Several previous studies have suggested that Hsp90 inhibitors could be applied to nononcological diseases as neuroprotective agents based on their induction of Hsps[22–28].

Androgen receptor (AR) is one of the Hsp90 client proteins[15], and is a pathogenic gene product of spinal and bulbar muscular atrophy (SBMA), one of the polyglutamine (polyQ) diseases[29]. This disease is characterized by premature muscular exhaustion, slow progressive muscular weakness, atrophy and fasciculation in bulbar and limb muscles[30]. PolyQ diseases are inherited neurodegenerative disorders caused by the expansion of a trinucleotide CAG repeat in the causative genes[31]. In SBMA, the number of polymorphic CAG repeats is normally 14–32, whereas it is expanded to 40–62 CAGs in the *AR* gene[32]. A correlation exists between CAG repeat size and disease severity[33]. The pathologic features of SBMA are motor neuron loss in the spinal cord and brainstem[30], and diffuse nuclear accumulation and nuclear inclusions of the mutant AR in the residual motor neurons and certain visceral organs[34].

We have already examined several therapeutic approaches in a mouse model of SBMA[35–38]. As a consequence, we confirmed that castration and leuprorelin, a luteinizing hormone–releasing hormone agonist that reduces testosterone release from the testis, substantially rescued motor dysfunction and nuclear accumulation of mutant AR in male transgenic mice[35,37]. Although this hormonal therapy was effective, it poses the unavoidable difficulty of severe sexual dysfunction[37]. In addition, this therapy cannot be applied to other polyQ diseases.

Here, we present a new and potent strategy for SBMA therapy with 17-AAG, an Hsp90 inhibitor. Given that Hsp90 inhibitors have two major activities, preferential client protein degradation and Hsp induction, we hypothesized that 17-AAG would degrade mutant AR more effectively than wild-type AR.

[1]Department of Neurology, Nagoya University Graduate School of Medicine, 65 Tsurumai-cho, Showa-ku, Nagoya 466-8550, Japan. [2]These authors contributed equally to this work. Correspondence should be addressed to G.S. (sobueg@med.nagoya-u.ac.jp).

Received 25 February; accepted 10 August; published online 11 September 2005; doi:10.1038/nm1298

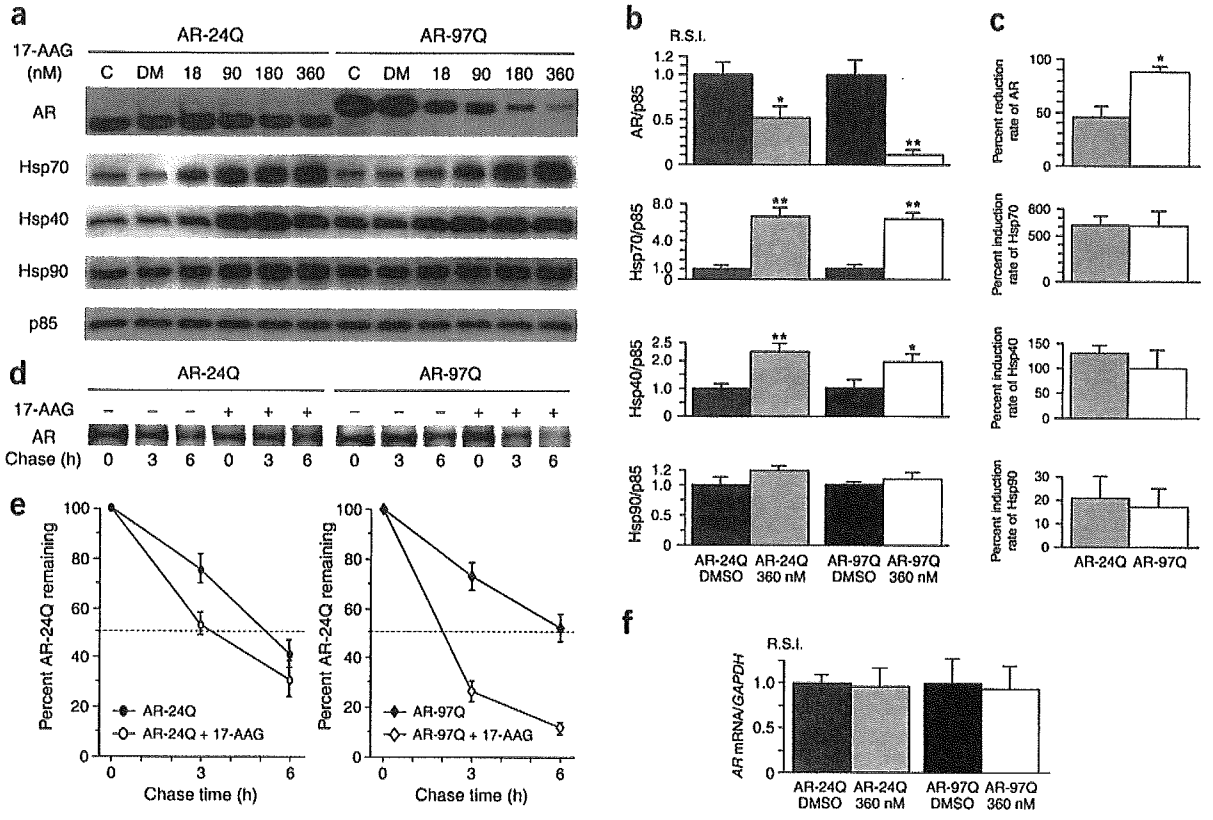

Figure 1 Effect of 17-AAG on the AR or chaperones in cultured-cell models. (**a**,**b**) Although the immunoblot and densitometric analysis showed a dose-dependent decline in both wild-type (AR-24Q) and mutant (AR-97Q) AR expression in response to 17-AAG, the mutant AR decreased more than did the wild-type. 17-AAG markedly increased the expression of Hsp70 and Hsp40, especially for Hsp70, but only slightly increased Hsp90 expression. (**c**) The decrease in mutant AR after treatment with 17-AAG was much higher than that of wild-type AR (88.9% versus 45.9%, $P = 0.0063$). Values are expressed as mean ± s.e.m. ($n = 5$). (**d**) Pulse-chase analysis of two forms of AR. Data from one representative experiment for wild-type and mutant AR. (**e**) Pulse-chase assessment of the half-life of wild-type and mutant AR. The amounts of AR-24Q and AR-97Q remaining in the absence and presence of 17-AAG are indicated. Values are expressed as mean ± s.e.m. ($n = 4$). (**f**) Real-time RT-PCR of wild-type and mutant *AR* mRNA. Quantities are shown as the ratio to *GAPDH* mRNA. The wild-type and mutant *AR* mRNA levels were similar under 17-AAG treatments. Values are expressed as mean ± s.e.m. ($n = 4$). $^*P < 0.025$, $^*P < 0.005$.

In this study, we examine the effects of 17-AAG on a cultured-cell model and the transgenic mouse model of SBMA. We show that the mutant AR exists more frequently as a stabilized Hsp90 chaperone complex than does the wild-type AR, and that 17-AAG selectively degrades the mutant AR. Administration of 17-AAG inhibits neuronal nuclear accumulation of the mutant AR and considerably ameliorates motor phenotypes of the SBMA model mouse.

RESULTS

Effect of 17-AAG on expression of AR and Hsps *in vitro*

To address the question of whether 17-AAG promotes the degradation of polyQ-expanded AR, we treated SH-SY5Y cells highly expressing the wild-type (AR-24Q) or mutant (AR-97Q) AR for 48 h with the indicated doses of 17-AAG or with DMSO as control. Although immunoblot analysis showed a dose-dependent decline in both wild-type and mutant AR expression after treatment with 17-AAG (**Fig. 1a**), the monomeric mutant AR decreased significantly more than did the wild-type ($P = 0.0063$; **Fig. 1b,c**), suggesting that the mutant AR is more sensitive to 17-AAG than is the wild-type. The expression of Hsp70 and Hsp40 were also markedly increased after treatment with 17-AAG, but Hsp90 was only slightly increased (**Fig. 1a,b**). There were no significant differences, however, in the levels of Hsp70, Hsp40 and Hsp90 induction between the wild-type and mutant AR (**Fig. 1c**).

To determine whether the decrease in AR resulted from protein degradation or from changes in RNA expression, we assessed the turnover of wild-type and mutant AR with a pulse-chase labeling assay. Without treatment, the wild-type and mutant AR were degraded in a similar manner, as previously reported[39,40]. In the presence of 17-AAG, however, the wild-type and mutant AR had half-lives of 3.5 h and 2 h, respectively (**Fig. 1d,e**), whereas levels of mRNA encoding the wild-type and mutant AR were quite similar (**Fig. 1f**). Cell viability did not differ between wild-type and mutant AR transfected cells (data not shown). These data indicate that 17-AAG preferentially degrades the mutant AR protein without cellular toxicity or alteration of mRNA levels.

To address why 17-AAG preferentially degrades mutant AR, we determined the levels of Hsp90, Hop and p23 associated with wild-type or mutant AR in SH-SY5Y cells without 17-AAG treatment (**Fig. 2a**). Hop and p23 are two essential components of multi-chaperone Hsp90 complexes[1]. Without 17-AAG treatment, coimmunoprecipitation from the cell lysates with antibodies to AR showed that p23 was more highly associated with mutant than with wild-type AR (**Fig. 2a,b**). The total levels of Hsp90, Hop and p23 were similar in the cells transfected with either wild-type or mutant AR (**Fig. 2a**).

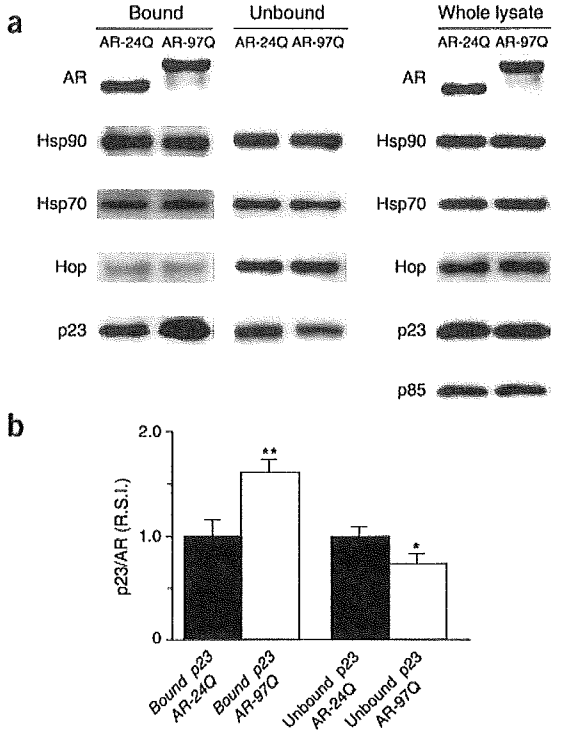

Figure 2 Immunoprecipitation of wild-type and mutant AR in cultured-cell models. **(a)** Wild-type and mutant AR were immunoprecipitated from cell lysates with an AR-specific antibody and immunoblotted with antibodies to the indicated western blot proteins. There was more mutant AR present in multichaperone complexes with p23 than there was wild-type AR. There were no differences in total expression levels of AR, Hsp90, Hsp70, Hop and p23 between wild-type and mutant AR–expressing cells. Control immunoprecipitations without antibodies did not immunoprecipitate any co-chaperones (data not shown). **(b)** The densitometric analysis of p23 in the bound and unbound fractions shows there was 1.6 times as much p23 associated with mutant AR than there was with the wild-type ($P < 0.01$). This experiment was repeated with five sets of cells with equivalent results. Values are expressed as mean ± s.e.m. ($n = 5$). $^{*}P < 0.05$, $^{**}P < 0.01$. R.S.I., relative signal intensity.

We next examined the status of the Hsp90 chaperone complex in wild-type and mutant AR-expressing cultured cells treated with 17-AAG. Immunoprecipitation with AR-specific antibody showed that Hsp90 chaperone complex–associated Hop was markedly increased, and p23 decreased depending on the dose of 17-AAG (**Fig. 3a,b**), suggesting that treatment with 17-AAG resulted in the shifting of the AR-Hsp90 chaperone complex from a mature stabilizing form with p23 to a proteasome-targeting form with Hop. The loss of p23 from the mutant AR-Hsp90 complex was significantly higher ($P < 0.005$) than that from the wild-type AR-Hsp90 complex (**Fig. 3c**). The degradation of wild-type and mutant AR by 17-AAG was completely blocked by the proteasome inhibitor MG132 (**Fig. 3d**), suggesting that the pharmacological degradation by 17-AAG was dependent on the proteasome system, as previously reported[17,18]. Furthermore, these results strongly suggest that mutant AR is more likely to be in the Hsp90-p23 multichaperone complexes, which eventually enhances 17-AAG–dependent proteasomal degradation of mutant AR.

Moreover, mutant AR was markedly decreased after treatment with 17-AAG even when induction of Hsp70 and Hsp40 was blocked by the protein-synthesis inhibitor cycloheximide (**Supplementary Fig. 1** online), suggesting that 17-AAG contributes to the preferential degradation of mutant AR mainly through Hsp90 chaperone complex formation and subsequent proteasome-dependent degradation rather than through induction of Hsp70 and Hsp40.

17-AAG ameliorates phenotypic expression of SBMA mice

We administered 17-AAG (2.5 or 25 mg/kg) to male transgenic mice carrying full-length human AR-24Q or AR-97Q. The disease progression of AR-97Q mice treated with 25 mg/kg 17-AAG (Tg-25) was

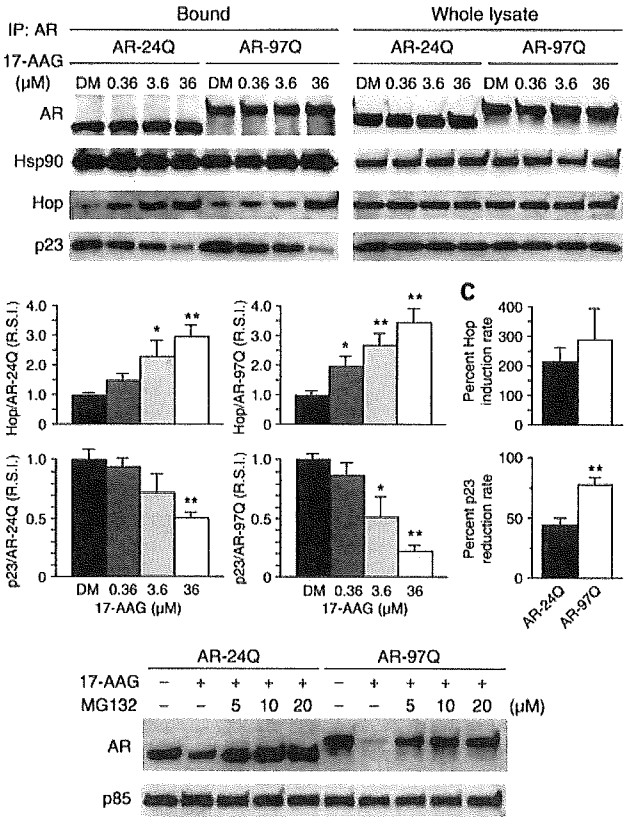

Figure 3 Pharmacological change in the AR-Hsp90 complex, and the correlation to proteasomal degradation. **(a)** Immunoblots of lysates of transfected cells treated with 17-AAG. Lysates were immunoprecipitated with AR-specific antibody. The short time exposure to 17-AAG did not decrease the amount of mutant AR. There were dose-dependent changes in both Hop and p23 after treatment with 17-AAG; however, no dissociation of Hsp90 from the mutant AR complex was seen. There were no changes in the expression of Hop, p23 and Hsp90 in whole lysates in the presence of 17-AAG. **(b)** Densitometric analysis of Hop and p23 in the bound fractions. There was a marked increase in the amount of Hop, and a marked decrease in p23 in both wild-type and mutant AR-bound Hsp90 complexes after treatment with 17-AAG. R.S.I., relative signal intensity. **(c)** Comparisons of induction rate of Hop and reduction rate of p23 in the Hsp90 complexes of wild-type and mutant AR. Although there was no significant difference in the induction rate of Hop between the wild-type and mutant AR complexes, the reduction rate of p23 was significantly higher in the mutant AR complex compared with that in the wild-type complex (43.8% versus 79.0%, $P < 0.005$). Values are expressed as means ± s.e.m. ($n = 5$). **(d)** Effect of 17-AAG on AR expression under the inhibition of proteasomal degradation. The mutant AR was more markedly reduced than wild-type AR after 17-AAG treatments; however, this pharmacological degradation was completely blocked by MG132 in both cases. DM, DMSO. $^{*}P < 0.025$, $^{*}P < 0.005$.

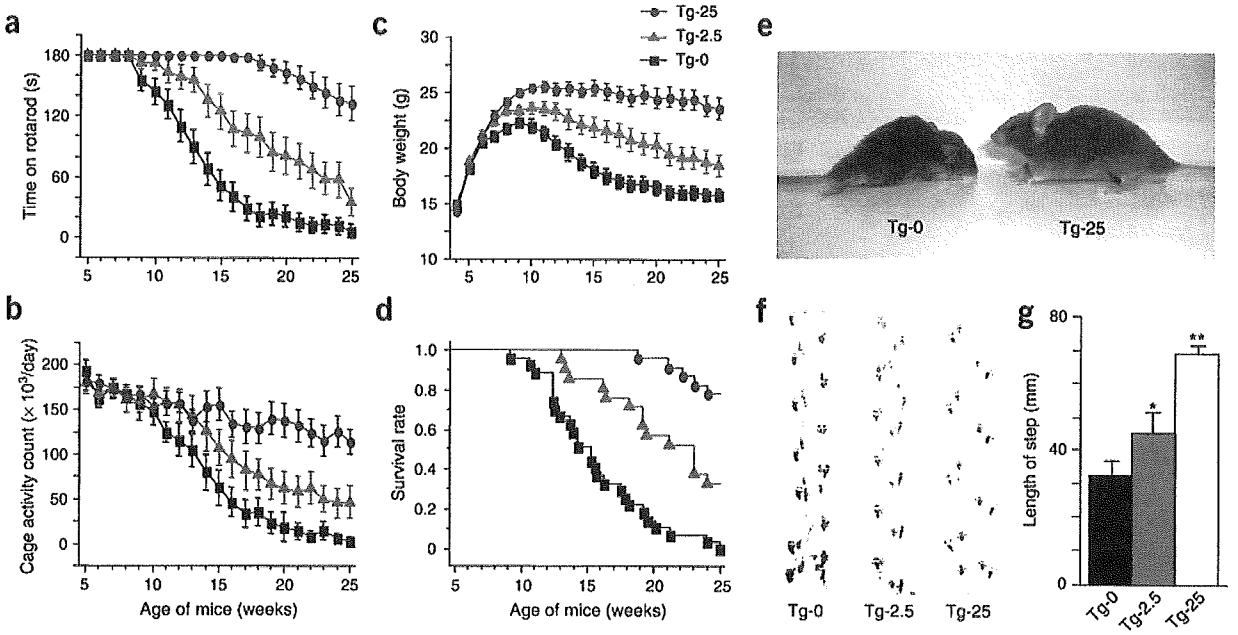

Figure 4 Effects of 17-AAG on behavioral and visible phenotypes in male AR-97Q mice. (**a**) Rotarod task ($n = 27$), (**b**) cage activity ($n = 18$), (**c**) body weight ($n = 27$) and (**d**) survival rate ($n = 27$) of Tg-0, Tg-2.5 and Tg-25 mice. All parameters were significantly different between the Tg-0 and Tg-25 ($P < 0.005$ for all parameters). A Kaplan-Meier plot shows the prolonged survival of Tg-2.5 and Tg-25 compared with Tg-0, which had all died by 25 weeks of age ($P = 0.004$, $P < 0.001$, respectively). (**e**) Representative photographs of a 16-week-old Tg-0 (left) shows an obvious difference in size, and illustrates muscular atrophy and kyphosis compared with an age-matched Tg-25 (right). (**f**) Footprints of representative 16-week-old Tg-0, Tg-2.5 and Tg-25 mice. Front paws are indicated in red and hind paws in blue. (**g**) The length of steps was measured in 16-week-old Tg-0, Tg-2.5 and Tg-25 mice. Each column shows an average of steps of the hind paw. Values are expressed as means ± s.e.m. ($n = 6$). $^*P < 0.025$, $^{**}P < 0.005$.

markedly ameliorated, and that of mice treated with the 2.5 mg/kg 17-AAG (Tg-2.5) was mildly ameliorated (**Fig. 4a–d**). The untreated transgenic male mice (Tg-0) showed motor impairment assessed by the rotarod task as early as 9 weeks after birth, whereas Tg-25 mice showed initial impairment only 18 weeks after birth and with less deterioration than Tg-0 mice (**Fig. 4a**). Tg-2.5 mice showed intermediate levels of impairment in rotarod performance (**Fig. 4a**). The locomotor cage activity of Tg-0 mice was also markedly decreased at 10 weeks compared with the other two groups, which showed decreases in activity at 13 (Tg-2.5) and 16 (Tg-25) weeks of age (**Fig. 4b**). Tg-0 mice lost weight significantly earlier and more profoundly than the Tg-2.5 ($P < 0.025$) and Tg-25 mice ($P < 0.005$; **Fig. 4c**). Treatment with 17-AAG also significantly prolonged the survival rate of Tg-2.5 ($P = 0.004$) and Tg-25 mice ($P < 0.001$) as compared to Tg-0 mice (**Fig. 4d**). 17-AAG was less effective at the close of 2.5 mg/kg than 25 mg/kg in all parameters tested. The lines were not distinguishable in terms of body weight at birth; however, by 16 weeks, Tg-0 mice showed obvious differences in body size, muscular atrophy and kyphosis compared to Tg-25 mice (**Fig. 4e**). Additionally, Tg-0 mice showed motor weakness, with short steps and dragging of the legs, whereas Tg-25 mice showed almost normal ambulation (**Fig. 4f,g**).

When we immunohistochemically examined mouse tissues for mutant AR using the 1C2 antibody, which specifically recognizes expanded polyQ, we observed a marked reduction in 1C2-positve nuclear accumulation in the spinal motor neurons (**Fig. 5a**) and muscles (**Fig. 5b**) of Tg-25 mice compared with those of Tg-0 mice. Glial fibrillary acidic protein (GFAP)-specific antibody staining showed an apparent reduction of reactive astrogliosis in Tg-25 compared with Tg-0 mice in the spinal anterior horn (**Fig. 5c**). Muscle histology also showed marked amelioration of neurogenic muscle atrophy in the AR-97Q mice treated with 17-AAG (**Fig. 5d**). We confirmed a significant reduction of 1C2-positive nuclear accumulation in both spinal cord ($P < 0.01$) and skeletal muscle ($P < 0.05$) by quantitative assessment (**Fig. 5e**). AR-24Q mice and normal littermates treated with 17-AAG showed no altered phenotypes (data not shown).

To evaluate the toxic effects of 17-AAG, we examined blood samples from 25-week-old mice treated with 25 mg/kg 17-AAG for 20 weeks. Measurements of aspartate aminotransferase, alanine aminotransferase, blood urea nitrogen and serum creatinine showed that treatment with 17-AAG resulted in neither infertility nor liver or renal dysfunction in the AR-97Q male mice at the dose of 25 mg/kg (**Supplementary Fig. 2** online).

Mutant AR is preferentially degraded by 17-AAG *in vivo*

As the mutant AR was preferentially degraded as compared to the wild-type AR in the presence of 17-AAG *in vitro*, we also examined the level of AR in the SBMA mouse model. Western blot analysis of lysates of the spinal cord and muscle of AR-97Q mice showed high molecular–weight mutant AR protein complex retained in the stacking gel as well as a band of monomeric mutant AR, whereas only the band of wild-type monomeric AR was visible in tissues from the AR-24Q mice (**Fig. 6a,b**). Treatment with 17-AAG notably diminished both the high molecular–weight complex and the monomer of mutant AR in the spinal cord and muscle of the AR-97Q mice, but only slightly diminished the wild-type monomeric AR in AR-24Q mice (**Fig. 6a,b**). Treatment with 17-AAG decreased the amount of the monomeric AR in AR-97Q mice by 64.4% in the spinal cord and 45.0% in the skeletal muscle, whereas these amounts were only 25.9% and 12.5%, respectively, in AR-24Q mice (**Fig. 6a,b**). Thus, the reduction rate of the monomeric mutant AR was significantly higher than the wild-type

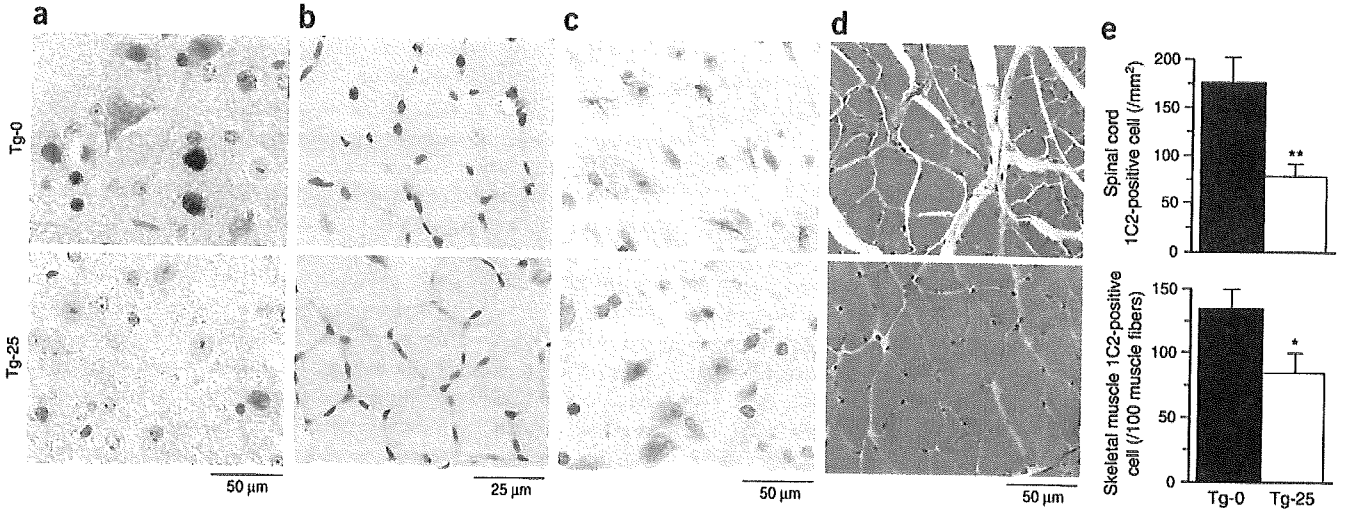

Figure 5 Effects of 17-AAG on the histopathology of male AR-97Q mice. **(a,b)** Immunohistochemical staining with 1C2-specific antibody showed marked differences in diffuse nuclear staining and nuclear inclusions between Tg-0 and Tg-25 mice in the spinal anterior horn and skeletal muscle, respectively. **(c)** Immunohistochemical staining with GFAP-specific antibody also showed an obvious reduction of reactive astrogliosis in the spinal anterior horn of mice treated with 17-AAG. **(d)** Hematoxylin and eosin staining of the muscle in Tg-0 mice showed obvious grouped atrophy and small angulated fibers, which were not seen in Tg-25 mice. **(e)** There was a significant reduction in 1C2-positive cell staining in the spinal cord ($P < 0.01$) and skeletal muscle ($P < 0.05$) in Tg-25 as compared to Tg-0 mice. Values are expressed as mean ± s.e.m. ($n = 6$). $^*P < 0.05$, $^{**}P < 0.01$.

AR in both spinal cord ($P < 0.001$) and skeletal muscle ($P < 0.01$; **Fig. 6c**). The levels of wild-type and mutant *AR* mRNA were similar in the respective mice treated with 17-AAG (**Fig. 6d**). We also performed filter-trap assays for quantitative analyses of both the large molecular aggregated and soluble forms of the mutant AR[36]. Both forms of trapped AR-97Q protein were markedly reduced in the spinal cord and muscle of Tg-25 mice, whereas those from the AR-24Q were not (**Supplementary Fig. 3** online). These observations strongly indicate that 17-AAG markedly reduces not only the monomeric mutant AR protein but also the high molecular–weight mutant AR complex, because of the preferential degradation of the mutant AR.

Western blot analysis showed that the levels of Hsp70 and Hsp40 in spinal cord were increased by 47.1% and 29.5%, respectively, and in muscle by 29.2% and 24.7%, respectively (**Supplementary Fig. 4** online) after treatment with 17-AAG. These pharmacological effects of chaperone induction were statistically significant ($P < 0.05$ for all parameters), but not as marked as the 17-AAG–induced mutant AR reduction, and were also not as pronounced as those arising from genetic manipulation in our previous study[36].

Hsp90 inhibitors nonspecifically activate heat shock responses through a dissociation of the heat-shock transcription factor (HSF-1) from the Hsp90 complex[27,41]. Although the expression of

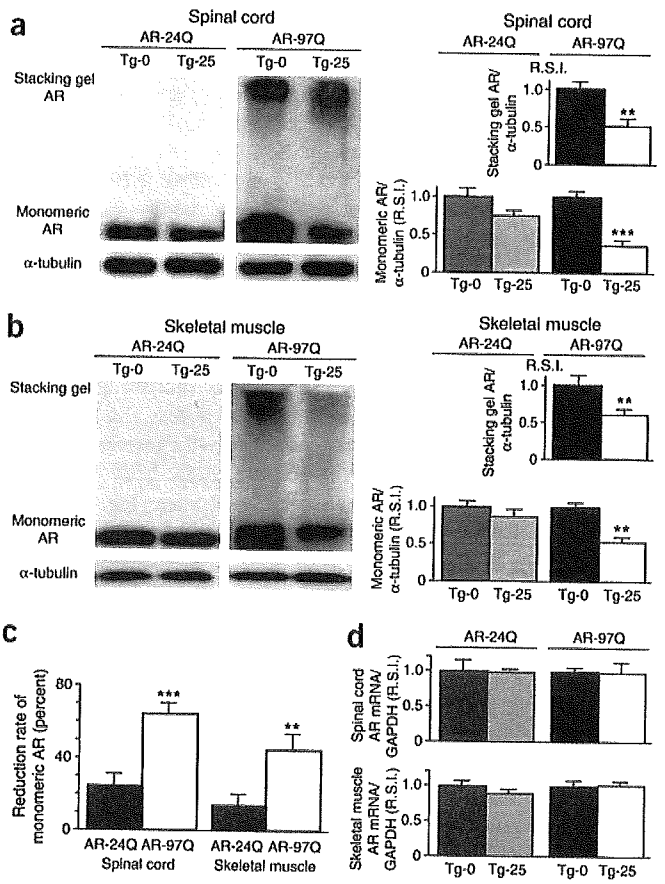

Figure 6 Effects of 17-AAG on AR expression in male AR-24Q or 97Q mice. **(a,b)** Western blot analysis of the spinal cord and muscle of AR-24Q and AR-97Q mice probed with AR-specific antibody. In both spinal cord and muscle of mice treated with 17-AAG, there was a significant decrease in the amount of mutant AR in the stacking gel and monomeric mutant AR in AR-97Q mice, but only slightly less monomeric wild-type AR in AR-24Q mice compared with that from untreated control mice. **(c)** Comparison of reduction rate of wild-type and mutant AR. Densitometric analysis showed that the 17-AAG–induced reduction of monomeric mutant AR was significantly greater than that of the wild-type monomeric AR. 17-AAG resulted in a 64.4% decline in monomeric mutant AR in the spinal cord, and a 45.0% decline in the skeletal muscle, whereas there was only a 25.9% decline in the spinal cord and a 12.5% decline in the skeletal muscle of AR-24Q mice. These results show significant differences of the reduction rate between wild-type and mutant AR in both spinal cord and skeletal muscle. Values are expressed as mean ± s.e.m. ($n = 5$). $^*P < 0.05$, $^{**}P < 0.01$, $^{***}P < 0.001$. **(d)** Real-time RT-PCR of wild-type and mutant *AR* mRNA *in vivo*. The expression levels of wild-type and mutant *AR* mRNA in transgenic mouse spinal cord and skeletal muscle were similar under 17-AAG treatments. Values are expressed as mean ± s.e.m. ($n = 3$).